Civil aviation and the environment – the next frontier for the aerodynamicist

J. E. Green
Aircraft Research Association
Bedford, UK

ABSTRACT

In the coming century, the impact of air travel on the environment will become an increasingly powerful influence on aircraft design. Unless the impact per passenger kilometre can be reduced substantially relative to today's levels, environmental factors will increasingly limit the expansion of air travel and the social benefits that it brings. The three main impacts are noise, air pollution around airports and changes to atmospheric composition and climate as a result of aircraft emissions at altitude. The lecture will review the work done within the Air Travel – Greener by Design programme to assess the technological, design and operational possibilities for reducing these impacts. The main aeronautical disciplines all have something to contribute but it is in aerodynamics that the greatest opportunities appear to lie. If these opportunities are pursued, the aircraft in production in 2050 could be very different from those of 2005. It is for the aerodynamicists, supported by the structures and systems engineers and the materials scientists, to make the case for a radical leap.

NOMENCLATURE

Symbols

A	aspect ratio (= b^2/S)
a, b	constants in Lanchester's drag formulation
b	wing span
c	dynamic similarity parameter proposed by Lanchester (= Reynolds number)
C_D	drag coefficient (= D/qS)
C_{DO}	drag coefficient at zero lift
C_f	skin friction coefficient (= $2\tau_W/\rho U^2$)
C_L	lift coefficient(= L/qS)
D	drag
D_i	induced drag
F	Lanchester's tangential force
g	gravitational acceleration
H	calorific value of fuel (energy per unit mass)
H	boundary-layer shape parameter (= δ^*/θ)
l	length scale used by Lanchester
L	lift
$(L/D)_M$	maximum lift/drag ratio
M	Mach number
p	static pressure
q	dynamic pressure (= $0{\cdot}7p\mathrm{M}^2$)
q_M	value of q at $(L/D)_M$
R	range
S	wing area
S_{DO}	drag area (= D/q) at zero lift
Th_S	specific thrust (= net thrust per unit mass of engine air flow)
u	streamwise velocity component within boundary layer
U	streamwise velocity at edge of boundary layer
v	velocity component normal to surface within boundary layer
v_S	suction velocity (= $-v_W$)
v_W	velocity at porous wall (positive away from surface)
V	flight velocity
V_1	flight velocity at maximum L/D

Received 15 June 2006
This paper is an adaptation of the 2005 Lanchester Lecture presented at The Royal Aeronautical Society, May 2005.

V_2	flight velocity at minimum power
W	aircraft weight in flight
W_E	aircraft empty weight
W_{MF}	weight of mission fuel
W_P	weight of payload
X	aircraft range parameter (= $H\eta L/D$)
x	streamwise distance in boundary layer
y	distance normal to surface in boundary layer
δ^*	boundary-layer displacement thickness
η	overall propulsive efficiency (= $\eta_{therm}\,\eta_{trans}\,\eta_{prop}$)
η_{therm}	engine thermal efficiency
η_{trans}	transfer efficiency
η_{prop}	propulsive efficiency of jet (Froude efficiency)
θ	boundary-layer momentum thickness
κ	vortex drag factor (unity for elliptically loaded wing)
λ	q/q_M
μ	absolute viscosity
ρ	density

Abbreviations

AeIGT	Aerospace Innovation and Growth Team
DOC	direct operating cost
EC	European Commission
EI(NO_X)	NO_X emission index (gm of NO_X emitted per kg of fuel burned)
GPS	global positioning system
HLFC	hybrid laminar flow control
HP	Handley Page
HS	Hawker Siddeley
IPCC	Intergovernmental Panel on Climate Change
LFC	laminar flow control
LP	low pressure
NACA	National Advisory Committee for Aeronautics
NACRE	New Aircraft Concepts Research (EC FP6 research programme)
NASA	National Aeronautics and Space Administration
NLFC	natural laminar flow control
NO_X	mixture of oxides of nitrogen, NO and NO_2, emitted by gas turbines
NPL	National Physical Laboratory
OPR	overall pressure ratio
RAE	Royal Aircraft Establishment
RF	radiative forcing
TET	turbine entry temperature

1.0 INTRODUCTION

This lecture is dedicated to a great man, Frederick William Lanchester. He was a polymath, at heart an engineer but a man of great versatility and exceptional physical insight who contributed in many fields. In his early 20s he developed an interest in flight and by 1892 had evolved a theory of aerodynamics. He was persuaded not to publish this, on the grounds that his theories in this 'outlandish' field would damage his reputation as an engineer. Instead, in 1893, he designed and built his first petrol engine. In 1894 this was installed in a boat designed by his brothers that took to the river in Oxford as, probably, the first all-British power boat. In the following year, again working with two of his brothers, he designed and built the first petrol-driven car in England. In the years that followed, Lanchester cars progressively established a reputation for engineering innovation, smoothness and quality which derived from Frederick's creativity and attention to detail. Some of the many advances in motor engineering that he introduced are listed in the 31st Lanchester Lecture[1] given by Ackroyd in 1991 and a fuller account can be found in Kingsford's biography of Lanchester[2].

From 1904 onwards, he was able to devote less time to Lanchester cars and return to his earlier interest in flight. Working in isolation, he produced two substantial publications[3,4] on aerodynamics and stability which were published in 1907 and 1908 respectively. He had completed this work before the first flight of a powered aircraft in England, by S. F. Cody at Laffans Plain near Farnborough in October 1908. Figure 1 is a photograph of Lanchester, slide-rule in hand, taken not long after these publications. In 1915, he published[5] a further development of the aerodynamic theory of his 1907 book (first formulated in 1892[3]) and in the following year published a book on the use of aircraft in warfare[6]. To quote Ackroyd[1],

"In the latter publication he proposed the N^2 law which bears his name, gave a mathematical demonstration of the benefits of concentration in attack, and cited Nelson's tactics at Trafalgar as an example of an earlier, intuitive application of the principles he was proposing. All this initiated the study of a subject known today as operational research. John Fletcher tells me that there is now a considerable literature in Japanese in which Lanchester's principles have been applied to marketing."

The breadth of his contribution was in fact recognised in the title of the first Lanchester lecture[7], given in 1958 by Theodore von Kármán, "*Lanchester's contributions to the theory of flight and to operational research*".

Since then, it has become usual for the Lanchester lecture to have an aerodynamic theme and the present lecture is no exception. Its context is the impact of civil aviation on the environment, through noise, air pollution around airports and the effect of flight at altitude on the atmosphere and on climate. The last of these is taken to be the most important and the lecture concentrates on the options available for reducing the effect, in particular the options for reducing fuel burn. Whilst improvements in operational procedures, reductions in aircraft weight and increases in propulsion efficiency all have a contribution to make, it is argued that aerodynamic advance, particularly in drag reduction, offers the greatest potential gain. And here we find that, in assessing the benefits and limitations, we are drawing on the concepts and relationships that Lanchester set out in those visionary publications of almost a century ago.

2.0 ENVIRONMENTAL IMPACTS

2.1 Air Travel – Greener by Design

Towards the end of the last century it was becoming evident that, in the century to come, the impact of air travel on the environment would become an increasingly important influence on the evolution of civil aviation. Unless the impact per passenger could be reduced substantially relative to present levels, environmental factors could be expected eventually to limit the expansion of air travel and the social benefit that it brings. Discussion of this question between the Director of the Royal Aeronautical Society and the Director General of the Society of British Aerospace Companies led to a decision to form a partnership between the two bodies to consider environmental issues. The partnership grew to include the British Air Transport Association, the Airport Operators Association and the DTI and, shortly thereafter, Air Travel – Greener by Design was launched at a meeting held at the DTI in March 2000.

The primary objective of Greener by Design was, and is, to assess and promote options for mitigating the environmental impact of aviation. At its inaugural meeting, it formed three sub-groups to address operations, technology and market-based options. I have been the chairman of the Technology Sub-Group since March 2000 and of the re-formed Science and Technology Sub-Group since 2004.

The Technology Sub-Group adopted as its remit the impact of subsonic air travel on noise and air quality around airports and on the atmosphere and climate. It did not consider supersonic air travel, air traffic management (covered by the Operations

Table 1
Lifetimes of the main greenhouse gases and their precursors

Carbon dioxide	50 – 200 years
Methane	8 – 10 years
Water	weeks
Ozone	months
NO_x	weeks
Contrails/cirrus	hours

Sub-Group) or the environmental impact of aircraft manufacture and disposal (small compared to the through-life impact of operating the aircraft). The Sub-Group's first report was published in July 2001 and re-published[8] in the February 2002 issue of *The Aeronautical Journal*. It reviewed the past developments, current situation and future prospects in the three main areas of environmental impact: noise; local air quality near airports; and climate change. Of these three, the Sub-Group agreed at an early stage that impact on climate is the most important long-term problem and the content of the report reflects this. In 2004 the Sub-Group re-formed, in response to a request from the Aerospace Innovation and Growth Team (AeIGT), with the remit to review present understanding of the environmental impact of aviation and to make recommendations to the AeIGT on future research priorities. This work was completed early in 2005†. Again, impact on the atmosphere and on climate was considered the most important threat to air travel in the long term and the report reflects this.

In the first report there was a section entitled 'Facts of Life', which discussed the realities which have to be kept in mind in any discussion of the future evolution of civil aviation. The air transport industry, whilst it has a history of innovation and technological leadership, must nevertheless exercise prudence in both the technical and commercial arenas. Both the airline and aircraft industries operate in a highly regulated, highly competitive environment where margins are small, investment costs are high, many years are required to achieve a satisfactory return on investment and, above all, passenger safety is paramount. These factors tend to mitigate against radical changes in aircraft design and operation. There is however another reality, termed in the first report 'The Laws of Physics', which can be thought of as setting an upper bound to what can be achieved in aircraft performance. It is a bound that can be approached only by a radical departure from today's aircraft design standards and, in considering its aerodynamic aspects, we find that one of the most fundamental constraints was set out by Lanchester in 1907.

2.2 The main environmental impacts

The three main environmental impacts of civil aviation are the effect of noise on communities around airports, the effect of aircraft emissions in the vicinity of airports on local air quality and the effect of emissions at altitude on the atmosphere and on climate. An objective evaluation of their relative importance is not easy but it was attempted in a discussion paper[12] issued jointly by the Department for Transport and the Treasury in 2003. This estimated the annual external costs to the UK of its civil aviation as:

Noise	£25m
Local air quality	£119m – £236m
Climate change	£1,400m

These figures are roughly in inverse proportion to public perception, as measured by letters of complaint received by officials and members of parliament. Consequently, whilst impact on climate is arguably the most important issue in the long term, public concerns about noise and local air quality are likely to continue to inhibit growth in air travel and to require the attention of the operators, the manufacturers and the research community for some time to come.

Figure 1. Frederick William Lanchester, 1868 – 1946.

There are opportunities for researchers in aerodynamics and fluid mechanics to contribute both to the reduction of aircraft noise and to the reduction in the emission of NO_x (the oxides of nitrogen NO and NO_2) which is the main aircraft-generated threat to health near airports. To discuss research in these in any detail here would be a digression but they are considered at greater length in Refs. 8 and 9 and, in addition, Ref. 9 contains an appendix listing relevant research programmes in Europe and the USA.

3.0 CLIMATE CHANGE

3.1 The effect of aviation on climate

For every tonne of kerosene burned by an aircraft in cruise, approximately three tonnes of CO_2, 1·2 tonnes of water vapour and 14kg of NO_x are exhausted into the atmosphere (the mass of NO_x in the exhaust depending on the characteristics of the combustion chamber). These constitute more than 99·9% of the combustion products, the other significant ingredients being small quantities of CO, soot and oxides of sulphur. Each of the three main constituents has a significant impact on climate.

There is considerable debate about the most appropriate metric for characterising the effect on climate of these emissions. In its major report of 1999[13], the Intergovernmental Panel on Climate Change

† The draft report was completed before the Lanchester lecture but not published until July 2005. It was re-published as Ref. 9 in the September 2005 issue of *The Aeronautical Journal*.

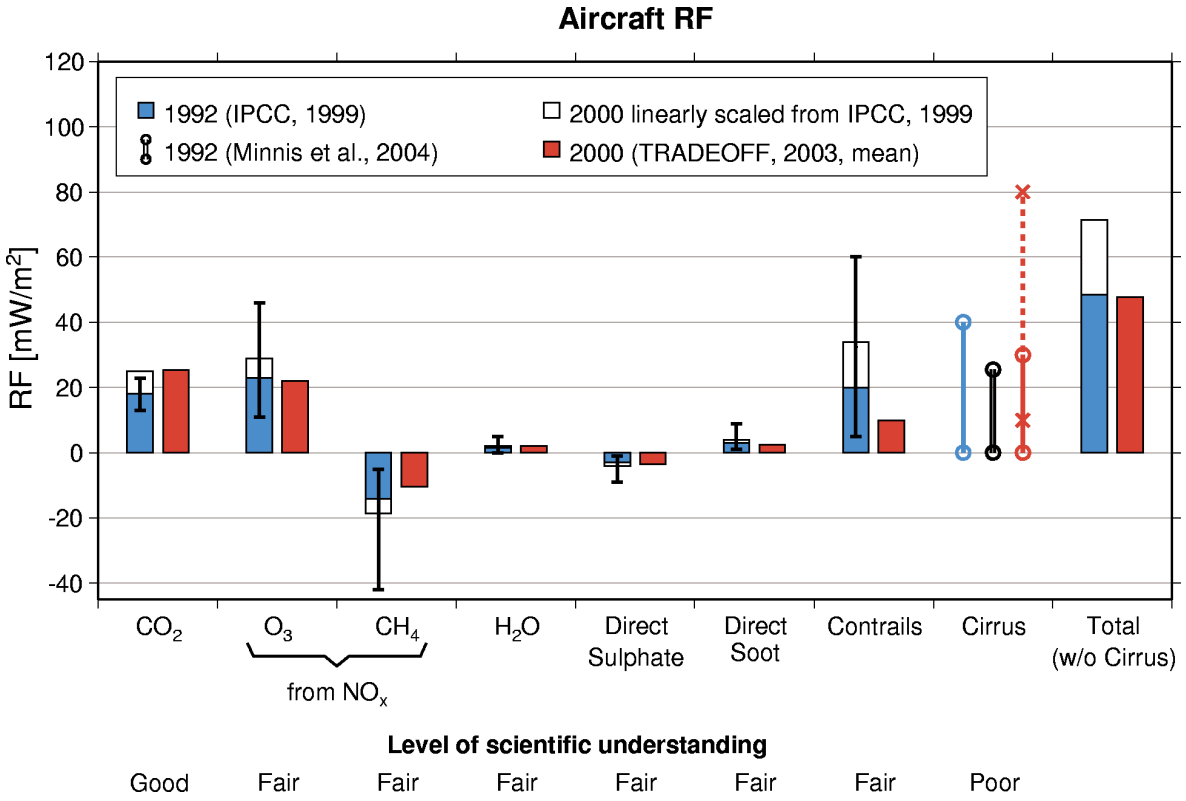

Figure 2. Radiative Forcing from aircraft in 1992 and 2000 (TRADEOFF, 2003).

(IPCC) discussed the issue at length and opted for radiative forcing (RF). This is a measure of the perturbation at the tropopause, expressed in W/m^2, of the energy balance between incoming solar radiation and outgoing long wavelength radiation from the earth and the atmosphere. It was adopted also in the recent, EC funded TRADEOFF study[14], in which estimates of the contributions to the RF from aviation in 2000 were compared with the IPCC[13] estimate for 1992. Figure 2, taken from Ref. 14, shows this comparison. The whiskers on the figure indicate the 2/3 confidence limits of the IPCC estimates for 1992. No such limits are shown for the TRADEOFF estimates but a qualitative indication of the level of scientific understanding of the effect of each contributor is shown below the figure. Only for CO_2 is the scientific understanding considered good. Understanding of the other contributors is considered fair except for cirrus cloud, for which it is considered poor.

Although the nitrogen oxides in NO_X are not greenhouse gases, their emission at altitude results in the creation of ozone (O_3) and the destruction of methane (CH_4), both of which are strong greenhouse gases. Water and CO_2 are both greenhouse gases and condensation trails, which are clouds of ice particles formed from the water vapour in the engine exhaust, also have a greenhouse effect. In addition cirrus cloud, formed from the evolution over time of persistent contrails, is thought to be a significant contributor – possibly the most substantial contributor of all. Table 1 on the preceding page, taken from Rogers *et al*[15], shows the lifetimes of the main greenhouse gases and precursors.

In the sections which follow, measures are noted which suggest that there is greater potential to reduce the impact of ozone (by reducing NO_X) and of contrails and contrail cirrus than of CO_2. However, because CO_2 has such a long life in the atmosphere, it is vital in the long term to achieve a substantial reduction in CO_2 emissions also.

The scientific uncertainties indicated below Fig. 2, coupled with doubts about RF as a metric, prevent an accurate evaluation of the relative importance of these emissions. This presents particular problems in cases where action to reduce the effect of one emission can increase the effect of another. To quote Ref. 9, "Lack of a robust understanding of the nature and magnitude of the effects of aircraft emissions impedes aircraft designers and policy makers alike in addressing the question of how best to minimise the future environmental impact of air travel". That said, there are in effect only three significant contributors – contrails/cirrus, NO_X and CO_2 – and they require quite different measures to reduce their impact. These are considered in turn below.

3.2 Contrails and contrail-induced cirrus cloud

Figure 3 shows a sky crossed by three persistent contrails, behind which lie bands of cirrus cloud which at some previous time may, or may not, have been contrails. The poor level of understanding of cirrus noted under Fig. 2 reflects three uncertainties: the extent of aviation-induced cirrus; the radiative efficiency of this cirrus; and the relative extents of primary, contrail-induced cirrus and secondary cirrus arising from aircraft generated particles and aerosols. The estimates by TRADEOFF[14] in Fig. 2 are based on statistical analyses of cloud and air traffic patterns and do not distinguish between primary and secondary cirrus. However, Ref. 14 does cite the study by Mannstein and Schumann[16], who estimated that the cover by contrail cirrus in central Europe was approximately ten times larger than the cover by contrails. From Fig. 2 it is evident that, if this estimate were to be upheld, and to apply worldwide, the radiative impact of contrail cirrus would substantially outweigh that of the other contributors.

The evidence for secondary cirrus is unclear, as are the technological options for reducing it should it prove to be significant. For persistent contrails and cirrus which derives from persistent contrails, however, the situation is relatively clear. Persistent contrails form only in cold, moist air – air which is supersaturated with respect to ice. For an aircraft flying through supersaturated air, there is no technological possibility of preventing contrail formation. On the other hand, elimination of contrail and contrail cirrus formation can be assured by routing all air traffic to fly below, above or around ice-saturated regions.

Such diversionary tactics would increase fuel burn, and hence CO_2 and NO_X emissions, and would disrupt flight schedules. Avoiding all contrail formation would therefore not be an environmental optimum. Williams *et al*[17] have reported a study of reducing contrail formation in Europe by setting a limiting flight altitude which is varied at six hourly intervals to suit the prevailing meteorological conditions. From this it was estimated that reductions in contrail formation in the range 65% – 95% could be achieved at a cost in increased fuel burn in the range 2% – 7%. At present we do not understand the atmosphere well enough to determine where the best balance lies in the trade off between contrail formation and CO_2 and NO_X emission. Perhaps, by the time advances in air traffic management and meteorology have made operations of this kind practicable, understanding of the atmosphere will have reached the point where we can assess the emissions trade-off with reasonable confidence.

3.3 NO_X emission at altitude

There are three possible ways of reducing the impact on climate of NO_X emissions at altitude: reduce fuel burn; reduce EI(NO_X), the mass of NO_X emitted per unit mass of fuel burned; and reduce cruise altitude. The last of these is not yet established beyond question but more than one study[18,19] has suggested that, over the typical cruise altitude range, the impact of NO_X increases with altitude. For example, Ref. 8 "...found the modifications in the ozone impact to be strongly dependent on height and season. A reduction in flight altitude is likely to result in a reduction in the aircraft-induced total ozone column increase at most times of the year." Reducing cruise altitude would increase fuel burn for current aircraft but, if the reduction in NO_X impact is found to be substantial, future aircraft could be optimised for lower cruise altitude. The fuel burn penalty for a lower altitude design would be substantially less than the penalty of operating today's aircraft at the lower altitude.

Of the other two options, reducing fuel burn is discussed more fully below and reducing EI(NO_X) by advances in engine combustor technology and changes in engine design is discussed more fully in Ref. 9. Here it is sufficient to note that, in the light of recently completed and ongoing European technology demonstrator programmes, substantial reductions in EI(NO_X) are foreseen within the next 10 to 20 years.

4.0 FUEL BURN

For kerosene fuelled aircraft, emissions of the third contributor to climate change, CO_2, are directly proportional to fuel burn. And because fuel burn is an important component of operating costs, reducing it has been a priority for aircraft and engine designers since the beginning of the jet age. As a result, fuel burn per passenger kilometre has fallen by 70% over this period and the classic swept-winged, turbofan-powered aircraft has become a highly developed machine with limited scope for further increases in fuel efficiency.

Even so, reducing fuel burn is a high commercial as well as an environmental priority and is likely to remain so for the foreseeable future. Also, in the context of climate change, it is worth noting that, with the exception of some aspects of engine design, all measures which reduce fuel burn reduce CO_2 and NO_X emissions in equal proportion.

Figure 3. Persistent contrails and cirrus cloud.

4.1 The Breguet range equation

The term 'fuel burn', which has been used in a rather general way up to this point, is intended to mean the mass of fuel burned divided by the product of the payload and length of flight (payload-range). It can be determined from the Breguet Range Equation. Whilst the equation does not quite have the status of the Second Law of Thermodynamics, it is an absolutely robust statement of one of the 'Laws of Physics' referred to in 2.1 which define the bounds of what is achievable in aircraft performance.

In Appendix A of Ref. 8 a form of the Breguet Range Equation was derived which can be cast as an expression for fuel burn per unit payload-range. The equation assumes continuous cruise-climb so as to maintain the aircraft at its optimum cruise condition and includes an allowance for the fuel burned during taxiing, climb to cruise altitude and en-route manoeuvring. If we write W_{MF} for the mission fuel burned between engine start-up and shut-down, W_E for the aircraft empty weight, W_P for the payload and R for the range, then from the form of the equation obtained in Appendix A of Ref. 8 we can derive

$$\frac{W_{MF}}{RW_P} = \frac{(1+W_E/W_P)(1\cdot022\exp(R/X)-1)}{R} \qquad \ldots (1)$$

where X is a range performance parameter defined by

$$X = H\eta L/D \qquad \ldots (2)$$

where H is the calorific value of the fuel, η is the overall propulsion efficiency of the engine and L/D is the lift-to-drag ratio of the aircraft at cruise. It is usual to express H in Joules/kg but, since this has the dimension length, H can also be expressed in km. Since η and L/D are dimensionless, X is then expressed in km. For a kerosene-fuelled medium- or long-range swept-winged aircraft with currently achievable values of η and L/D, X is approximately 30,000km.

4.2 Measures to reduce fuel burn

For an aircraft with a given payload, there are five independent variables on the right hand side of the equation: R, W_E, H, η and L/D. For a kerosene-fuelled aircraft, H is essentially fixed and we are left with four variables through which we can influence fuel burn. The first three of these, along with some operational measures, are considered briefly below.

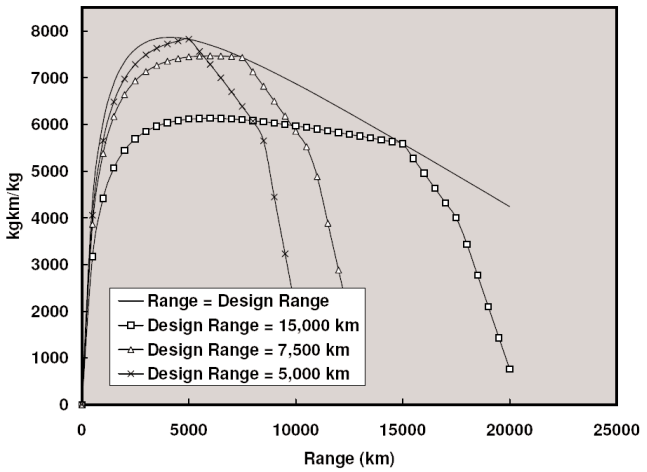

Figure 4. Payload fuel efficiency versus range and design range: swept-winged kerosene-fuelled aircraft.

4.2.1 Range

The range over which an aircraft operates, and the maximum range for which it is designed, both influence its fuel efficiency. Figure 4, taken from Ref. 8, shows payload fuel efficiency RW_P/W_{MF} (the reciprocal of the quantity given by Equation (1)) plotted against range for swept winged aircraft of today's technology standard. The outer curve is the design range envelope of fuel efficiency based on maximum payload, the inner curves show the variation with operating range of the fuel efficiency of aircraft of particular design ranges, again based on maximum payload.

Figure 4 shows that a medium-range aircraft, designed for a maximum range of around 4,000km, is appreciably more fuel efficient than a long-range aircraft. In Ref. 8 this was discussed at length and a worked example was put forward, suggesting that undertaking long-distance travel in medium-range aircraft, with one or two refuelling stops en-route, offered reductions of the order of 30% in fuel burn and in the empty weight (and cost) of the aircraft. A full system study of multi-stage long distance journeys was called for in Ref. 8 and the recommendation was repeated in Ref. 9.

Since then, Nangia[10] has provided evidence that the fuel burn per passenger-kilometre in a long-range aircraft is twice that of a medium range aircraft and the present author[11] has confirmed that his findings and Nangia's differ because of an error in Ref. 8 in the derivation of the structural weight constants used in the performance analysis. A worked example in Ref. 11, with revised structural weight constants, suggests that an aircraft designed to carry a given passenger load over 15,000km burns twice as much fuel as, and has twice the empty weight and two and a half times the take-off weight of, an aircraft designed to carry the same passenger load over the same distance in three stages. The difference between the conclusions of Refs 8 and 11 arise mainly from the fact that, for modern long range aircraft, the maximum passenger load is not much more than half the maximum payload. References 10 and 11 are in this issue of *The Aeronautical Journal*.

4.2.2 Operational measures

In Equation (1) the range R is the distance flown, rather than the great-circle distance, between the points of arrival and departure. The coefficient 1·022 of the exponential term on the right hand side of the equation is a simplification which includes an allowance for fuel burned in climbing to cruise altitude and in en-route manoeuvres. Routes which depart appreciably from great circle routes, for example to divert around military zones, and stacking at busy airports, which add to other en-route manoeuvres, increase fuel burn. Improvements in air traffic management, which are expected to recover some of this wasted fuel, are discussed in Ref. 9, as are two other, more speculative operational possibilities for reducing fuel burn.

The first is air-to-air refuelling, which would enable a medium range aircraft to undertake non-stop long distance flights, thereby achieving the savings in aircraft weight (and cost) and fuel burn discussed in 4.2.1 above. The second is formation flying, in the manner of migrating geese. Autonomous formation flying, using GPS to provide positional information, has been demonstrated by NASA and fuel savings of the order of 10% are projected for a formation relative to an isolated aircraft. The saving arises because following aircraft in the formation position themselves in the rising air from the trailing vortex of the aircraft ahead. In terms of Equations (1) and (2), the saving arises because the lift to drag ratio of the formation is higher than that of a single aircraft.

4.2.3 Aircraft empty weight

Options for reducing aircraft weight were discussed at length in Ref. 9. Many possibilities were identified, from reducing cruise Mach number to changes in the certification rules to allow reduced structural reserve factors. Two fields of advance from which weight savings can confidently be expected are (a) structural design and optimisation and (b) manufacturing processes.

The most clear cut opportunity for weight reduction is the replacement of structural aluminium with carbon fibre composite and other lightweight structural materials. The benefits of this will be seen in the Boeing 787 and the Airbus A350 and in Ref. 9 a projection to 2020 suggests that use of composite materials would give production aircraft of that date a fuel burn advantage of 10% – 15% over their year 2000 counterparts. As noted in Ref. 9 however, and in 4.2.1 above, for long- range aircraft an appreciably greater saving in weight and fuel burn can be achieved by redesigning them as medium range aircraft (which, for an existing type, means stretching the aircraft to increase payload and reduce fuel load within a given maximum take-off weight).

4.2.4 Propulsion efficiency

The overall propulsion efficiency in Equation (2) can be written

$$\eta = \eta_{therm}\,\eta_{trans}\,\eta_{prop} \qquad \ldots (3)$$

where η_{therm} is the thermal efficiency of the gas turbine, η_{trans} is the transfer efficiency (product of the efficiency of the fan and of the turbine driving it) and η_{prop} is the propulsive efficiency, sometimes known as the Froude efficiency. If the specific thrust of the engine (the net thrust divided by the total air mass flow through the engine in kg/kg/s) is Th_S and the aircraft is flying at velocity V, the ideal propulsive efficiency of a turbofan engine is closely approximated by

$$\eta_{prop} = \frac{1}{(1 + gTh_S/(2V))} \qquad \ldots (4)$$

where g is the gravitational acceleration. This equation shows that propulsive efficiency increases as flight speed increases and specific thrust decreases. For an aircraft cruising at Mach 0·85 at the tropopause, with engines having a specific thrust of 12kg/kg/s in cruise, typical of today's standard, the propulsive efficiency in Equation (4) is 84%. Typically, the transfer efficiency η_{trans} lies between 85 and 88% and the thermal efficiency η_{therm} is around 55%, giving an overall efficiency around 40% on an advanced engine today.

Of the three components in Equation (3), the transfer efficiency is already high and further increases are likely to be small, the fan and the low pressure turbine both being not far from the limits of achievable efficiency in turbo-machinery.

As Fig. 5 taken from Birch[20] shows, the thermal efficiency of the gas generator has increased appreciably since the 1960s, the

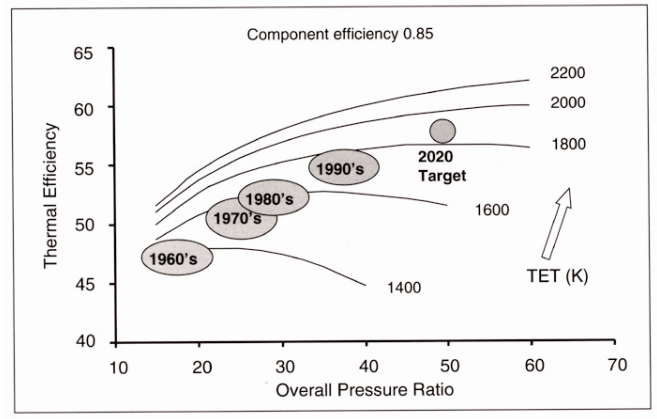

Figure 5. Gas turbine thermal efficiency.

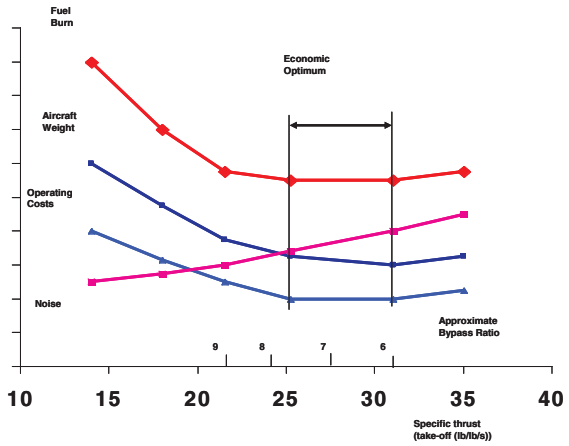

Figure 6. Variation of fuel burn, noise and weight with specific thrust.

advances each decade deriving from an increase both in overall engine pressure ratio (OPR) and in turbine entry temperature (TET). It is clear from the form of the curves of constant TET that further increase in thermal efficiency requires a further increase in both TET and OPR. Birch discusses in detail some of the difficulties of achieving these increases without losing the gains through secondary losses. The practical limits of achievable efficiency are discussed more fully in Ref. 9, where it is also noted that increases in both TET and OPR increase the rate of NO_X formation in the combustion chamber. It follows that an engine optimised to minimise impact on climate will have a lower TET and OPR than one of the same technology standard optimised to minimise fuel burn, as shown in the study by Whellens and Singh[21]. The difference in fuel burn between future engines optimised for these two different objectives will depend on the design standard of the combustor and on other possible NO_X reducing technologies noted in 3.3 above and discussed in Ref. 9. To the extent that advances in technology reduce EI(NO_X), the difference in fuel burn between the two forms of optimisation is likely to be smaller than that predicted in Ref. 21.

From Equation (4) we see that propulsive or Froude efficiency increases as specific thrust reduces or bypass ratio increases. However, as is seen in Fig. 6, also taken from Birch[20], there is an economic optimum level below which further reduction of specific thrust leads to increase in fuel burn, aircraft weight and operating costs. Specific thrust is reduced by increasing fan diameter, so as to increase the mass of air passing through the engine for a given thrust. This increases the weight of the low pressure (LP) system (fan and LP turbine), the weight and drag associated with the nacelle, and also increases the weight and loss of performance associated with integrating the engines with the airframe. For a turbofan engine, moving the economic optimum to lower values of specific thrust requires advances in materials and/or structural design to enable engine and nacelle weight to be reduced, and also aerodynamic advances, possibly including some form of boundary-layer control, to reduce nacelle and installation drag.

Some of the weight and drag penalties arising from the nacelle can be avoided by dispensing with it and adopting an open rotor design (with single or contra-rotating propellers). This offers significantly higher propulsive efficiencies, in excess of 90%, but at the expense of increased noise. For medium sized commercial aircraft, a compact high-efficiency design with contra-rotating propellers is the most promising option, provided acceptably low noise levels can be achieved.

Aerodynamicists will have contributions to make in the fields of nacelle and installation drag and in the development of more efficient, quieter open rotor propulsion. The main opportunity for advance, however, is by improving the aerodynamic efficiency of the airframe. This is the theme of the remainder of the lecture.

5.0 AERODYNAMIC EFFICIENCY

The final term in Equation (2) is the lift to drag ratio *L/D* – the aerodynamic efficiency of the airframe. This was a subject close to Lanchester's heart from the outset. Figure 7 is a photograph of Lanchester with a rubber-powered model aircraft taken in 1894, two years after he first formulated his aerodynamic theory. The wing has an aspect ratio of 13 and an elliptical planform.

Referring to Lanchester's discussion of this planform in his book on aerodynamics[3], Ackroyd[1] says, '*As to his choice of planform geometry, Lanchester provides a rather speculative but perceptive argument for this on the basis that, from the point of view of reducing aerodynamic resistance, it is better not to have the kinetic energy of the trailing vortices concentrated at the tips but spread out along the span of the wing'*. He ends with the comment that bird wings have '*...ordinates that approximate more or less closely to those of an ellipse.' Presumably the planform of the 1894 wing was obtained on this basis.*'

In 1913, Lanchester reported[22] that tests on a three-quarter scale model of this wing produced the highest lift to drag ratio then known, 17·1 at 4° incidence. This is not far below the best of the civil aircraft now in service. The theoretical result that the induced drag of a wing in inviscid flow is a minimum when the spanwise distribution of loading is elliptical did not appear until Prandtl published[23] the results of work at Göttingen in 1918.

5.1 Maximising *L/D*

In his 1907 book[3] Lanchester sets out models of the processes by which an aircraft generates lift and drag. He was the first person to perceive the role of the trailing vortex system created by a lifting wing of finite span. Intuitively, by 1897 it is believed[1], he developed a model which led to an expression for the induced drag D_i of a finite wing in inviscid flow. He calls this 'aerodynamic resistance' and argues that it takes the form $D_i \propto L^2/V^2$ where L is lift and V is flight velocity.

He also sets out models for drag. For the viscous drag of laminar flow over a plate he correctly proposes that the tangential force $F \propto V^{3/2}$. He then goes on to consider dynamic similarity, citing the experiments of Reynolds[24] on the onset of turbulent flow in pipes (Fig. 8), as evidence that '$V = c\mu/\rho l$ ... may be taken as the general

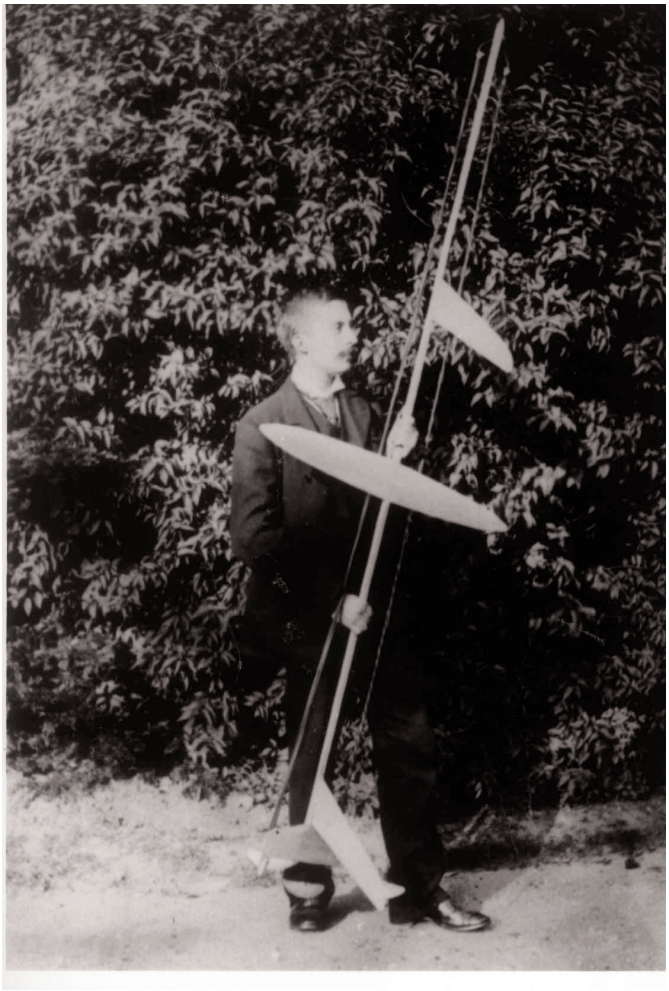

Figure 7. Lanchester in 1894 with rubber powered model aircraft.

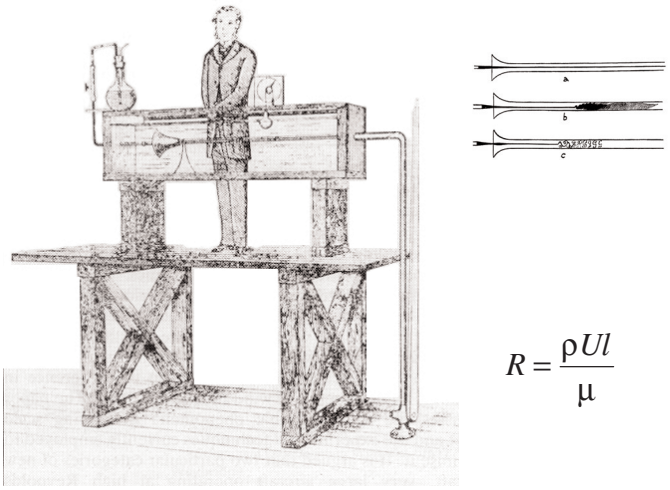

Figure 8. Osborne Reynolds in 1883 demonstrating transition from laminar to turbulent in water flow through a glass tube.

equation connecting all similar systems of flow in fluids.' Here, in effect, he has defined c as the Reynolds number for a body of characteristic dimension l and declared that geometrically similar bodies at the same Reynolds numbers will have identical flows (in Ref. 1 von Kármán is cited as attributing the first use of the term Reynolds number to the German physicist Sommerfeld in 1908). For aircraft, over which the boundary layer will be turbulent, Lanchester considers precedents for taking the friction force to vary with powers of V between 3/2 and 2 and finally, arguing that on an aircraft of that time there are significant regions of separated flow, he takes the view that a relationship of the form $F \propto V^2$ might well be adequate for practical applications to flight. The force F he terms 'direct resistance', as distinct from the 'aerodynamic resistance' of the preceding paragraph.

Adding his expressions for 'direct resistance' and 'aerodynamic resistance', Lanchester states that the total resistance must take the form

$$D = aV^2 + b/V^2 \qquad \ldots (5)$$

This relationship, of key importance in optimising aircraft performance, appeared for the first time in history in Lanchester's 1907 book and he followed it by analysis to show that an aircraft must have a minimum drag speed V_1, given by

$$V_1 = \left(\frac{b}{a}\right)^{1/4} \qquad \ldots (6)$$

at which the direct and induced drags are equal. In addition, he showed that an aircraft has a minimum power speed V_2 at which the induced drag is three times the direct drag, and that $V_1 = 3^{1/4}\, V_2$.

In modern terminology, Lanchester's deduction is that L/D is a maximum when the profile drag and lift dependent drag are equal. His drag formulation, Equation (5), is now classically written

$$C_D = C_{DO} + \frac{\kappa C_L^2}{\pi A} \qquad \ldots (7)$$

where C_{DO} is the drag coefficient at zero lift, C_L is the lift coefficient, κ is the so-called vortex drag factor, A is the aspect ratio and π is π (i.e.~22/7). This definition invokes the wing area S to define the drag and lift coefficients and perforce includes the aspect ratio as a key parameter. Following the same path as Lanchester, maximum L/D can be shown to occur when the two components of drag are equal, and to be given by

$$\left(\frac{L}{D}\right)_M = \sqrt{\frac{\pi A}{\kappa C_{DO}}} \qquad \ldots (8)$$

Corresponding to Lanchester's minimum drag speed, given by Equation (6), we now have a flight condition for maximum L/D at a dynamic pressure q_M given by

$$q_M = \sqrt{\frac{\kappa C_L^2}{\pi A C_{DO}}} \qquad \ldots (9)$$

In Section 4.2.2.3 of Ref. 8 alternative expressions were derived, avoiding wing area and aspect ratio, by writing

$$D = qS_{DO} + \frac{\kappa}{\pi q}\left(\frac{W}{b}\right)^2, \qquad \ldots (10)$$

where b is the wing span, S_{DO} is the drag area at zero lift (= SC_{DO}) and κ is again the vortex drag factor. Equating the two drag components gives the maximum lift to drag ratio in the form

$$\left(\frac{L}{D}\right)_M = b\sqrt{\frac{\pi}{4\kappa S_{DO}}} \qquad \ldots (11)$$

Figure 9. The Proactive Green aircraft of the EC NACRE programme.

at a flight condition given by

$$q_M = 0{\cdot}7\,pM^2 = W\sqrt{\frac{\kappa}{\pi b^2 S_{DO}}} \qquad \ldots (12)$$

where p is static pressure at the flight altitude, M is Mach number, W is aircraft weight and suffix M denotes conditions at maximum *L/D*. Since κ is slightly above unity and approximately constant for modern swept-winged aircraft, maximum *L/D* is proportional to the ratio of two lengths, the span and the square root of the zero-lift drag area, and the dynamic pressure at the flight condition for maximum *L/D* is proportional to a loading based on the product of these two lengths.

We see from Equation (11) that maximum *L/D* can be increased by increasing wing span or by reducing vortex drag factor and zero-lift drag area. It is worth noting in passing that increasing *L/D* by increasing b will reduce q_M and hence increase optimum cruise altitude or reduce optimum cruise Mach number. Increasing *L/D* by reducing κ or C_{DO} will have the reverse effect.

It is also worth noting that, in the overall optimisation of an aircraft design, taking account of factors such as the influence of cruise altitude on engine weight and hence on payload, it is usual to design for a cruise altitude somewhat lower than that for maximum *L/D*, giving a cruise *L/D* lower than the maximum. If the aircraft operates at a dynamic pressure q greater than q_M and we write

$$q = \lambda q_M \qquad \ldots (13)$$

L/D is then given by

$$\frac{L}{D} = \left(\frac{L}{D}\right)_M \frac{2}{(\lambda + 1/\lambda)} \qquad \ldots (14)$$

which varies relatively slowly for values of λ around unity. For example, for a value of λ of 1·25, corresponding to flight at the design Mach number at an altitude approximately 5,000ft below the altitude for maximum *L/D*, the value of *L/D* given by Equation (14) is 2·5% below the maximum.

Aircraft designed for relatively short ranges may have broadly similar layouts to members of the same family designed for longer ranges, and not greatly different maximum values of *L/D*, but may have appreciably lower values of *L/D* at cruise. The factors governing the choice of cruise *L/D* for a particular aircraft are discussed at length by Kuchemann[25], Chapter 4.

5.2 Options for increasing maximum *L/D*

Of the three options for increasing $(L/D)_M$ that are offered by Equation (11), two are discussed briefly hereunder before we consider the third.

5.2.1 Increasing wing span

Since Equation (11) shows maximum *L/D* to be directly proportional to wing span, increasing span would seem an obvious candidate for increasing *L/D*. However, current long-range aircraft are optimised to minimise fuel burn at current cruise Mach numbers and on a successful design the balance between wing span and wing weight is close to optimum. An increase in span would require strengthening of the inboard wing to carry the increased bending moments and the resulting increase in wing weight would more than offset the benefit of the increase in *L/D*.

Some possible ways of increasing span without a weight penalty are discussed in Ref. 9, including a reduction cruise Mach number to allow reduced sweep and/or thicker wing sections and the use of advanced composite wing skins to reduce weight, both measures leading to an optimised wing with greater span. Reference 9 also notes the Proactive Green aircraft in the EC FP6 NACRE programme, Fig. 9, which among other things will explore the potential for increasing span to achieve higher *L/D*.

5.2.2 Reducing vortex drag factor

The so-called vortex drag factor κ of today's classic swept-winged configuration is about 1·20 at cruise. The minimum possible value of κ is 1·0 for an elliptically loaded wing in isolation in inviscid flow.

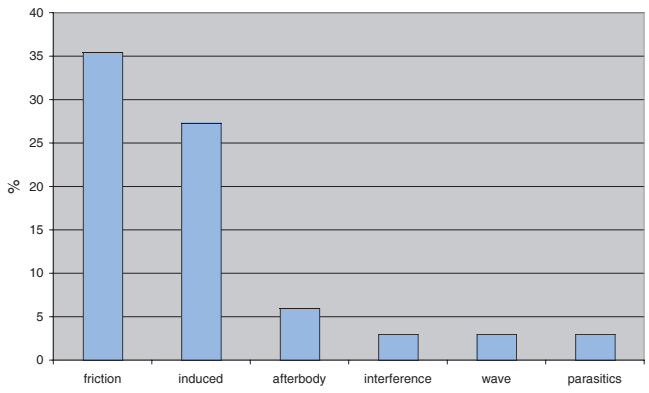

Figure 10. Drag breakdown typical of a large modern swept-winged aircraft.

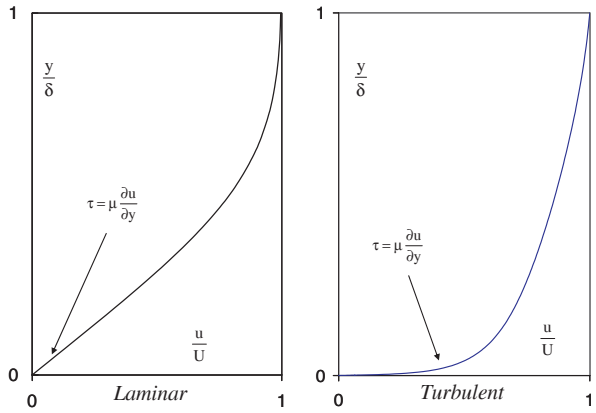

Figure 11. Laminar and turbulent boundary-layer velocity profiles.

In fact, the factor κ has become used to account for two drag components. The major one is the lift-induced drag, manifest as energy dissipated in the trailing vortex system from the wings, the minor one is the lift-dependent part of the profile drag, arising from increased boundary-layer growth on the wing caused by the lifting pressure distribution on the aerofoil. Both components vary as the square of the lift. For a modern swept-winged aircraft, the profile drag component accounts for the greater part of the departure of κ from unity and the prospect for a significant reduction in κ by improved aerodynamic design is small.

Further, as Prandtl showed in 1933, the classical elliptical distribution of span loading of the wing does not produce the most fuel-efficient result. It is advantageous to skew the elliptical distribution so as to carry less lift on the outer wing, thereby reducing wing bending moments and wing weight. The optimum value of κ will therefore always be greater than 1·0.

After discussing potential ways of reducing κ, Ref. 9, recalling from Equation (11) above that maximum *L/D* varies inversely as the square root of κ, concludes that the potential for increasing *L/D* by reducing κ is strictly limited.

The third option from Equation (11) for increasing maximum *L/D* is to reduce the zero-lift drag area S_{DO} – the profile drag of the aircraft. This is more promising territory.

6.0 PROFILE DRAG

Figure 10, derived from Marec[26], shows the drag breakdown of a typical transport aircraft at cruise. The two main components are the friction drag, which in Fig. 10 includes the wing pressure drag at subcritical conditions, and the lift-induced drag. The remaining components – afterbody, interference, wave and parasitic – are all relatively small. It is difficult to envisage how they might be reduced significantly without some penalty in terms of weight or cost, though some possibilities are discussed in Ref. 9.

In particular, in the case of wave drag, it is worth noting that, because propulsive efficiency increases with flight speed (Equation (4)), the most fuel-efficient cruise Mach number is part way up the drag rise, where the rate of increase of wave drag with Mach number just offsets the rate of increase in propulsive efficiency. An aircraft cruising at its most fuel efficient will always have a finite wave drag.

6.1 Laminar and turbulent boundary layers

In 1883 Reynolds[24] demonstrated (Fig. 8) the occurrence of laminar and turbulent flows in pipes and identified a dimensionless quantity, now termed Reynolds number, which characterised the boundary between one type of flow and the other. In his book of 1907[3], Lanchester discussed laminar and turbulent flow over external surfaces and argued that Reynolds number was the condition for dynamic similarity. He also proposed the boundary-layer concept – he termed it 'inert layer' – independently of and possibly ahead of Prandtl's seminal publication[27] on the subject in 1904, and at the time of writing his 1907 book he was evidently unaware of Prandtl's work. There is a good discussion of Lanchester's formulation of the concept, his analysis of laminar and turbulent friction drag and his insight into boundary-layer separation, in Ackroyd[1].

The boundary layer is the thin layer of fluid close to the surface of a body in which the fluid velocity is reduced from the velocity of the free stream at the edge of the boundary layer to zero at the wall. Figure 11 shows characteristic velocity profiles through laminar and turbulent boundary layers in flows at constant pressure. The ordinate is distance *y* from the wall scaled by the boundary-layer thickness δ, the abscissa is velocity *u* scaled by the velocity *U* at edge of the boundary layer – the free stream velocity. The turbulent boundary layer has a very thin region close to the wall – the so-called viscous sub-layer – in which the flow is laminar. Hence, as shown on the figure, the shear stress τ at the wall in both flows is given by

$$\tau = \mu \frac{\partial u}{\partial y} \qquad \ldots (15)$$

where μ is the absolute viscosity.

The velocity profile of the turbulent layer is much fuller than its laminar counterpart and the velocity gradient $\partial u/\partial y$ at the wall, when scaled by *U* and δ, is evidently very much greater in the turbulent layer. Although turbulent boundary layers are generally much thicker than the laminar boundary-layers upstream of them, it is no surprise in the light of Fig. 11 that the shear stress τ at the wall – the skin friction – is substantially greater beneath the turbulent layer than in the upstream laminar flow.

Figure 12 shows a turbulent velocity profile again, together with the two integrands from which the two key integral parameters of the boundary layer, displacement thickness δ^* and momentum thickness θ are derived†. Displacement thickness is the measure of the displacement of the free stream away from the surface as a result of boundary-layer growth. Momentum thickness is a measure of the combined pressure and friction drag of the surface. The definitions of these integral parameters are retained downstream of the aircraft and, in the case of a two dimensional aerofoil in a flow without shockwaves, the momentum thickness is a measure of the drag of the aerofoil.

† For simplicity, the definitions shown are for incompressible flow. For compressible flow, the definitions include terms in density.

6.2 Transonic flow over an aerofoil with turbulent boundary layers

The profile of a typical transonic aerofoil, together with its pressure distribution at the design point, is sketched in Fig. 13. The pressure is shown with suction ($-C_p$) plotted upwards. The area within the pressure loop gives the lift on the aerofoil and it is worth noting that a sizeable fraction of the lift comes from the last 40% of chord – the so-called rear loading arising from the downward camber of the rear of the aerofoil.

In the region of high suction over the forward part of the aerofoil the flow is supersonic, this being terminated by the shock wave at about 55% chord, after which there is a short region of re-acceleration followed by a steep deceleration, ie a steep rise in pressure, which is sustained all the way to the trailing edge. It is a feature of rear loaded aerofoils that there is a similar region of steep deceleration on the under surface between about 45% and 80% chord, though this is then followed by a region of re-acceleration up to the trailing edge. The character of the upper and lower surface pressure distributions determines the profile drag of the aerofoil.

The development of momentum thickness over the upper and lower surfaces of this aerofoil at a typical flight Reynolds number (30 million) is shown in Fig. 14. At the trailing edge the thickness on the upper surface is some 2·8 times that on the lower surface, though at mid-chord the two thicknesses are similar. From about 45% chord, where momentum thicknesses on the two surfaces are equal, that on the upper surface grows by a factor of about seven compared with a factor of 2·5 on the lower surface, the growth on both surfaces being dominated by pressure gradients. The result is that almost three quarters of the profile drag comes from boundary-layer growth on the upper surface.

The growth of momentum thickness over the aerofoil can be predicted by the boundary-layer momentum integral equation, first derived by von Kármán. In its original form, for incompressible, two-dimensional flow, the equation is usually written

$$\frac{\mathrm{d}\theta}{\mathrm{d}x} = \frac{C_f}{2} - \frac{\theta}{U}(H+2)\frac{\mathrm{d}U}{\mathrm{d}x} \qquad \ldots (16)$$

where C_f is the skin friction coefficient and H ($= \delta^*/\theta$) is the velocity profile shape parameter. The second term on the right hand side, involving the velocity gradient $\mathrm{d}U/\mathrm{d}x$, is the dominant term over the rear of the aerofoil on both surfaces and accounts for the steep increase in θ over the upper surface evident in Fig. 14.

An alternative way of writing the equation for compressible flow is

$$\frac{\mathrm{d}}{\mathrm{d}x}\left(\rho U^2\theta\right) = \delta^*\frac{\mathrm{d}p}{\mathrm{d}x} + \tau_w \qquad \ldots (17)$$

where ρ is density in the free stream, p is pressure and τ_w is shear stress at the wall. In this form, the equation sets out clearly the two components of aerofoil profile drag. The term on the left hand side is the streamwise rate of growth of momentum deficit in the boundary layer, the first term on the right hand side is the local contribution to the aerofoil pressure drag and the second term is the local contribution to friction drag.

The chordwise distribution of these two terms for the aerofoil of Figs 13 and 14 is shown in Fig. 15. Skin friction is dominant over the first half of the chord, pressure drag over the second half. There is a sudden increase in the pressure drag term through the shock, followed by a small negative contribution in the falling pressure downstream of the shock and then a steadily increasing contribution in the pressure rise up to the trailing edge. From Equation (16) we can see that, when the term in $\mathrm{d}U/\mathrm{d}x$ is large compared to the skin friction term, the rate of growth of momentum thickness is proportional the local thickness. Hence, to a first approximation, the rising pressure over the rear of the aerofoil simply amplifies the momentum deficit at mid chord that has been created by skin friction over the forward part of the aerofoil. It is this feature of the flow behaviour which makes laminar flow control a worthwhile proposition for transonic aerofoils.

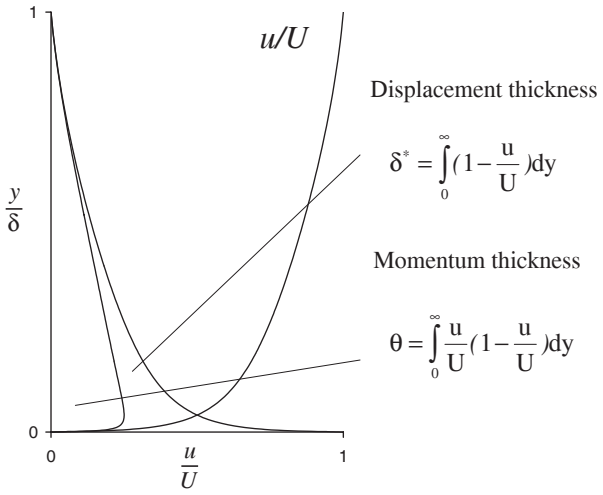

Figure 12. Boundary layer integral thicknesses.

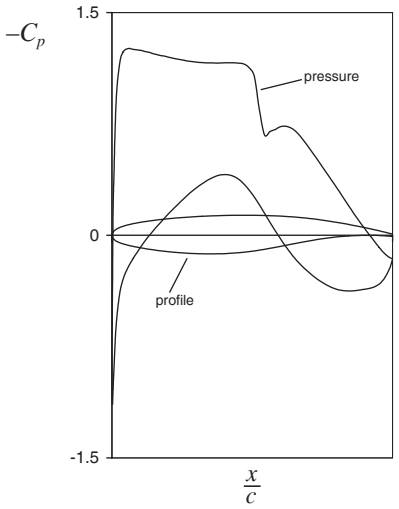

Figure 13. Transonic aerofoil profile and pressure distribution with fully turbulent boundary layers.

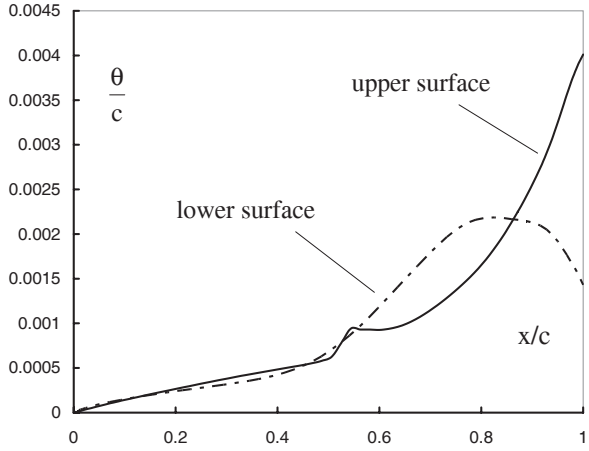

Figure 14. Momentum thickness growth on a transonic aerofoil with fully turbulent boundary layers.

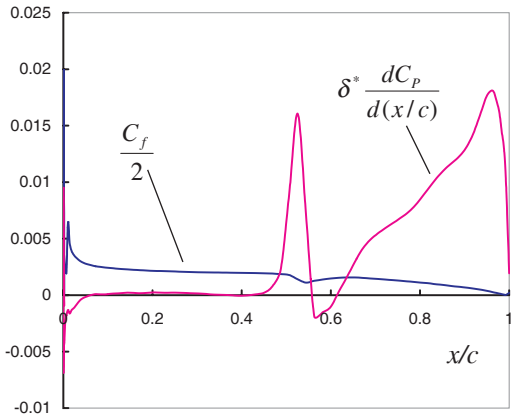

Figure 15. Pressure drag and skin friction components on the upper surface of a transonic aerofoil with turbulent boundary layers.

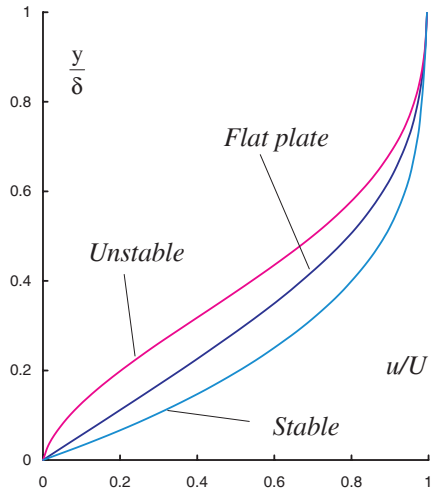

Figure 16. Stable and unstable velocity profiles in a laminar boundary layer.

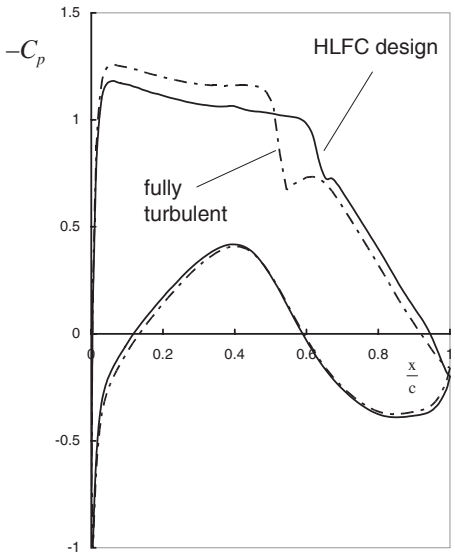

Figure 17. Pressure distributions on hybrid laminar flow control (HLFC) aerofoil at design and fully turbulent conditions.

6.3 Reducing profile drag by laminar flow control

Profile drag can be reduced by delaying or preventing the transition of the boundary layer from laminar to turbulent. There are three types of Control, Natural Laminar Flow Control (NLFC) and Hybrid Laminar Flow Control (HLFC), both of which delay transition – ie move the transition location rearwards on the aerofoil – and what is termed here full laminar flow control, which seeks to maintain a laminar boundary-layer over virtually the entire surface.

On swept-winged aircraft there are three distinct mechanisms which trigger transition and which have to be understood and, if necessary, suppressed to achieve any form of laminar flow control. The first, which can occur in a two-dimensional laminar boundary layer, is usually termed the Tollmien-Schlichting instability. The basic instability was first predicted by Lord Rayleigh in 1880[28] but it was not until 1929 that Tollmien[29] showed the role of viscosity in determining stability limits. The second, which can occur close to the attachment line at the leading edge of a swept wing, is termed cross-flow instability and was shown by Owen and Randall[31] to be an inviscid instability that arises if the cross-flow velocity profile of the boundary layer has an inflection point. The third trigger is termed leading-edge contamination – the promotion of transition locally by incoming turbulence convected along the leading edge from a turbulent boundary-layer upstream, as from a fuselage or wing root. This phenomenon was first encountered in flight experiments on laminar flow in the USA and the UK at about the same time[32,33,34] and the criterion for its onset was subsequently confirmed in wind tunnel tests by Poll[35].

Today, the measures needed to avoid leading-edge contamination are well understood and the other two types of instability can be modelled satisfactorily for aerodynamic design purposes by linear stability theory[36] and, if necessary, suppressed by boundary-layer suction as discussed for example by Wong and Maina[37] and Schrauf[38]. Since my purpose is to discuss only the basic nature of the constraints facing the aerodynamic designer, I shall consider only the nature and suppression of the Tollmien-Schlichting instability in the two dimensional laminar boundary-layer.

This instability depends strongly on the shape of the velocity profile. Figure 16 shows three characteristic velocity profiles in a laminar boundary-layer. The central one, labelled 'flat plate', is the profile obtaining in flows with zero pressure gradient. Its form was derived by Blasius[39] in 1908. Its curvature $\partial^2 u/\partial y^2$ is everywhere negative, approaching zero asymptotically in the limits $y \to 0$ and $y \to \infty$. The curve which has negative curvature at the wall is labelled 'stable' and that with positive curvature at the wall 'unstable'. In fact, the unstable feature of this third profile is not so much the positive curvature at the wall but the consequential existence of an inflection point in the profile.

Rayleigh had shown in 1880 that, in inviscid flow, the absence of an inflection point in a profile was a necessary condition for small disturbances not to be amplified – i.e. for the flow to be stable. Tollmein[29] showed that in a viscous flow, whilst the effect of viscosity at low Reynolds numbers is to damp out small disturbances, at higher Reynolds numbers these disturbances can be amplified even for profiles which do not have an inflection point. Pretsch[40] subsequently calculated neutral stability curves for a range of velocity profiles characteristic of accelerating and decelerating flows, including flow at constant pressure, defining boundaries within which disturbances within a specific range of wavelengths can be amplified.

Neutral stability boundaries, and the rate at which small disturbances with wavelengths lying within the boundaries are amplified, are important subjects but beyond the scope of this lecture. It is sufficient here to note that the characterisation of the profiles in Fig. 16 is broadly correct. In decelerating flows, which have an inflection point in the velocity profile, transition occurs at appreciably lower Reynolds numbers than on a flat plate. For accelerating flows, with entirely convex velocity profiles, the reverse is the case.

6.3.1 Natural laminar flow control

Natural laminar flow control (NLFC) is not a recent invention. Its application in the design of the wing section for the P-51 Mustang gave that aircraft the range which made it an outstanding bomber escort in WW2. To explain it, we begin with the boundary-layer equations, first set out for incompressible laminar flow by Prandtl[27] in 1904

$$\text{Continuity} \quad \frac{\partial u}{\partial x}+\frac{\partial v}{\partial y}=0 \qquad \ldots (18)$$

$$\text{Momentum} \quad \rho u\frac{\partial u}{\partial x}+\rho v\frac{\partial u}{\partial y}=\frac{\partial \tau}{\partial y}-\frac{\mathrm{d}p}{\mathrm{d}x}=\mu\frac{\partial^2 u}{\partial y^2}-\frac{\mathrm{d}p}{\mathrm{d}x} \qquad \ldots (19)$$

Note that, whilst all other derivatives are partial, the pressure gradient term is ordinary, reflecting the boundary layer approximation that pressure can be assumed to be constant across the thickness of the layer. It is these equations which von Kármán integrated across the layer to derive Equation (16).

For flow over a solid surface both u and v are zero at the wall and Equation (19) becomes

$$\mu\frac{\partial^2 u}{\partial y^2}-\frac{\mathrm{d}p}{\mathrm{d}x}=0 \quad , \qquad \ldots (20)$$

an expression which Head[41] termed the first compatibility condition at the wall. We see from this that in accelerating flow (dp/dx negative) the velocity profile at the wall will be convex (negative curvature) and the stability of the layer will be increased. The greater the acceleration (expressed non-dimensionally in the form $\rho\theta^2(dU/dx)/\mu$), the greater the boundary-layer Reynolds number $\rho U\theta/\mu$ for which the layer will be stable to small disturbances.

For a lifting aerofoil it is of course not possible to have accelerating flow over the entire surface – after the region of suction there has to be a deceleration to bring the pressure at the trailing edge back to approximately the free stream level. However, by shaping the wing profile so as to maintain gently accelerating flow over the forward 50% or so of both upper and lower surfaces, it is possible to maintain laminar boundary layers over the forward wing and, thereby, reduce the pressure drag arising from rapid boundary layer growth in the decelerating flow over the rear. Reynolds number limits its applicability to small and medium-sized aircraft, the limiting size of aircraft falling as wing sweep is increased. For wings of low sweep, NLFC can be applied to aircraft slightly larger than the Airbus A320.

One study some 26 years ago by Boeing[42], in which two NLFC project designs were compared with a reference, all-turbulent design similar to a Boeing 727, concluded that combining the effects of an increase in wing span with the reduction in wing profile drag given by NLFC led to increases in L/D of 20% and 30% for the two project designs (in both cases, more than half the increase coming from the increase in span). These gains in L/D were offset, however, by growth in wing weight such that there was no significant reduction in fuel burn and the direct operating costs of both project designs were appreciably greater than for the reference all-turbulent aircraft. There have however been advances in aerodynamics, structures and materials applications since the Boeing report and a new design study now seems worth doing. The Proactive Green aircraft in Fig. 9 provides a suitable vehicle for such a design study.

6.3.2 Hybrid laminar flow control

Hybrid laminar flow control (HLFC) has the same objectives as NLFC, to maintain laminar flow over the forward half of the wing and thus reduce the pressure drag from boundary-layer growth in the rising pressure over the rear. By combining wing shaping with boundary-layer suction over the forward part of the wing, transition to turbulent flow can be delayed to higher Reynolds numbers and extensive laminar flow can be achieved on appreciably larger aircraft.

For flows with suction at the surface, either through porous material or through very small, closely spaced holes, the boundary condition at the wall in Equation (19) becomes $u = 0$, $v = v_w = -v_s$, where v_s is the local area-mean suction velocity, and from (19) the first compatibility condition at the wall can be written

$$\mu\frac{\partial^2 u}{\partial y^2}=\frac{\mathrm{d}p}{\mathrm{d}x}+\rho v_W\left(\frac{\partial u}{\partial y}\right)_W=\frac{\mathrm{d}p}{\mathrm{d}x}-\rho v_S\frac{\tau_W}{\mu} \qquad \ldots (21)$$

Thus flow acceleration and suction through the wall both give rise to a convex profile with increased stability.

A second, no less important effect of boundary-layer suction is that it reduces, and can halt or reverse, the rate of boundary-layer growth. For flows with suction, the von Kármán momentum integral equation, in the form of Equation (17), becomes

$$\frac{\mathrm{d}}{\mathrm{d}x}\left(\rho U^2\theta\right)=\delta^*\frac{\mathrm{d}p}{\mathrm{d}x}+\tau_W+\frac{v_W}{U} \quad =\delta^*\frac{\mathrm{d}p}{\mathrm{d}x}+\tau_W-\frac{v_S}{U} \qquad \ldots (22)$$

In the particular case of flow at constant pressure, uniform suction at the wall is capable of maintaining a laminar boundary indefinitely, the boundary layer approaching an asymptotic state in which $\tau_w = v_s/U$, momentum thickness is constant and the suction Reynolds number $\rho v_w\theta/\mu$ has a value of 0·5. Bussmann and Muntz[43] calculated the stability limit for this flow to be at a momentum thickness Reynolds number of approximately 35,000, some two orders of magnitude higher than for the Blasius flat plate boundary layer. Perhaps of more practical interest to the aircraft designer is the fact that Equation (21) shows that, by applying appropriate suction, a laminar boundary layer with a convex velocity profile can be maintained in a region of decelerating flow.

In fact, whilst most early modelling of wings with HLFC envisaged suction as an extension to the aerodynamic design concepts developed for NLFC, with suction supplementing the effect of gently accelerating flow over the forward part of the aerofoil, recent studies by Wong and Maina[37] have pointed in a different direction. Their work has shown that, for a given energy into the suction system, a greater performance benefit can be obtained for aerofoils with an adverse 'rooftop' pressure distribution, similar to that adopted for modern designs with fully turbulent boundary layers, rather than the flat or favourable pressure distributions that were traditionally thought appropriate for laminar flow applications.

Figure 13 shows the pressure distribution over a transonic aerofoil at a chord Reynolds number of 30 million with fully turbulent boundary layers. In Fig. 17 that is compared with the pressure distribution for an aerofoil with HLFC designed for the same lift coefficient and Reynolds number†. On the HLFC aerofoil the lift is carried more to the rear, the suction ($-C_p$) over the first half of the upper surface is lower and hence the Mach number ahead of the shock is lower, the shock is weaker and the drag arising from total pressure loss through the shock is lower.

In Fig. 18 the growth of the upper and lower surface momentum thicknesses for the two aerofoils are compared. For the HLFC aerofoil, suction is applied only to the forward 15% of the upper surface but its calculated effect is to delay transition to 40% chord. The effect is to reduce momentum thickness at the trailing edge by approximately a third. For both aerofoils, boundary layer development over the rear of the aerofoil is dominated by the pressure rise between entry to the shock and the trailing edge, momentum thickness increasing by a factor of seven or more over this distance.

Boundaries for laminar flow control, as set out by Schrauf and Kühn[45], are shown in Fig. 19 in the form of curves of leading edge sweep against mean chord Reynolds number defining the limits of NLFC and HLFC. The figure indicates the range of large-scale experiments that support the proposed boundary between NLFC and HLFC and shows the HLFC limit embracing the full flight envelope

† I am grateful to Peter Wong of ARA for providing these results, derived using the well validated BVGK aerofoil design code[44] as further developed at ARA to apply to aerofoils with suction.

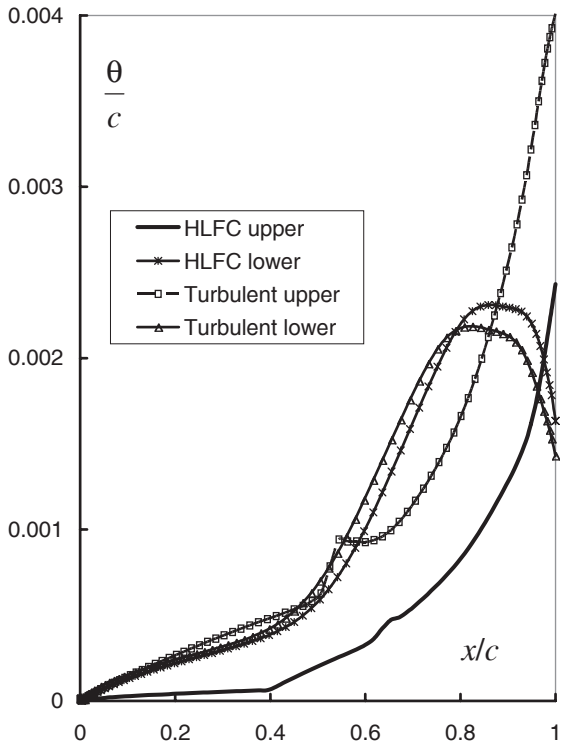

Figure 18. Momentum thickness growth on HLFC and fully turbulent aerofoils.

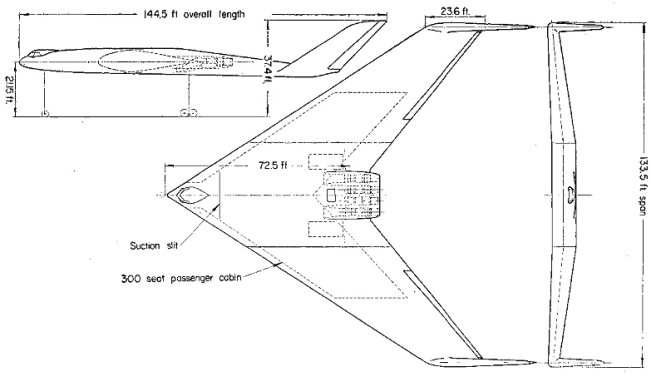

Figure 20. Handley Page HP-117 projected 300-seat laminar flow airliner.

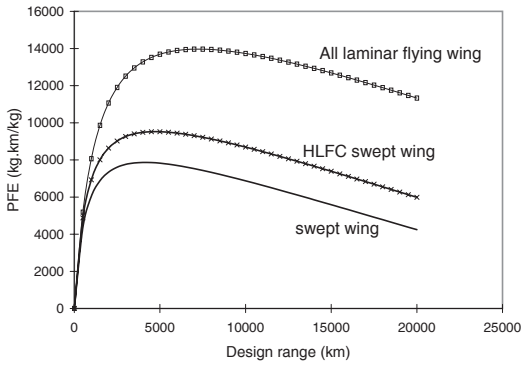

Figure 21. Variation of payload fuel efficiency with design range for kerosene-fuelled, turbulent and HLFC swept wing and laminar flying wing aircraft.

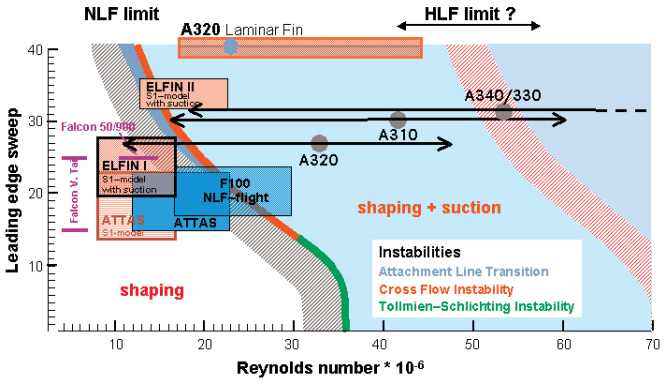

Figure 19. Limits of laminar flow control technologies.

Figure 22. The large blended wing-body of the EC NACRE programme.
©Copyright Airbus.

of the Airbus A310 and a substantial proportion of the A330/340 envelope. It also shows the reduction in limiting Reynolds number as sweep is increased to be proportionately much less for HLFC than for NLFC, making HLFC applicable to medium-sized aircraft with wing sweep of 30° or more. On the basis of current world traffic patterns, it is suggested in Ref. 9 that HLFC could be successfully applied to swept-winged aircraft over a range of sizes that accounts for roughly half the total world fuel burn.

The ability to achieve laminar flow by the application of suction over the forward part of a surface has been demonstrated in flight on an Airbus A320 fin and on a glove fitted to a Boeing 757 wing. There are many engineering and operational obstacles to be overcome[9] before either form of laminar flow control is adopted in the design of a new transport aircraft project, not least being the development of lightweight and efficient suction systems[37,38]. However, unlike the limits shown in Fig. 19, these are obstacles which can be addressed by engineering, they are not fundamental limits imposed by the 'Laws of Nature'.

6.3.3 Full laminar flow control

As Equation (21) shows, it is possible in a laminar boundary-layer to maintain a convex, stable velocity profile in a region of rising pressure by the application of suction, provided the suction term in the equation exceeds the pressure gradient term by a sufficient margin to ensure stability. In principle, therefore, it should be possible to maintain laminar flow through the pressure rise downstream of the peak suction on a lifting aerofoil, all the way to the trailing edge. Hence, it should be possible to construct an aircraft which has laminar flow over almost its entire surface.

Appreciation of this, and the fact that it had been confirmed experimentally in Germany in World War 2, led in the late 1940s to an upsurge of research into laminar flow and the possibilities of laminar flow aircraft. In the UK much of the drive came from Gustav Lachmann, Research Director at Handley Page Ltd, with work at the NPL, RAE and Cambridge University also contributing. In the USA the drive came from Werner Pfenninger at Northrop, supported by work at NACA Langley.

By around 1957 a considerable body of theoretical and experimental work had been created in both countries, including both wind tunnel and flight tests. In the UK, two de Havilland Vampire aircraft fitted with suction gloves over a wing upper surface, one at the Royal Aircraft Establishment and the other under Head at Cambridge University, had demonstrated laminar flow back to the trailing edge at Reynolds numbers of approximately 30×10^6. In the USA, Northrop had fitted a Lockheed F-94 Starfire with a part-span suction glove on a wing upper surface and had demonstrated full-chord laminar flow up to similar Reynolds numbers in well over 100 flights, including long distance flights between California and Dayton, Ohio.

Much of this work was summarised in 1961 in Volume 2 of the book *Boundary Layer and Flow Control* edited by Lachmann[46]. The book includes accounts of stability theory and laminar boundary layer prediction methods, of interest but now largely superseded, and also reports on much experimental work on such topics as suction surface geometry and construction, insect contamination and the fundamental aspects of propulsion for laminar flow aircraft.

The final contribution in the discussion of laminar flow, entitled '*Aspects of design, engineering and operational economy of low drag aircraft*', was provided by Lachmann himself and it is worth quoting from its introduction:

"It has been demonstrated both in the United Kingdom and in the United States that laminar flow over the full chord can be achieved in flight.

Jet fighter aircraft fitted with gloves to the wing to which suction was applied were used in both countries for these experiments which represented the culmination of many years' work on boundary layer control.

The state of the art which has been reached may be summarised as follows:

1. *Full chord laminar flow may be maintained in flight up to chord Reynolds numbers of the order of at least 36×10^6.*
2. *Suction quantities required to maintain laminar flow over straight wings are sufficiently small to result in net profile drag reduction of the order of from 70 to 80 percent, account being taken of the power required for suction.*
3. *Increase in Mach number at least up to the critical value has no adverse effect on the maintenance of laminar flow.*
4. *The tolerable degree of surface roughness and waviness of the outer skin for a given Mach number increases with cruising altitude in view of the corresponding increase in kinematic viscosity. Equally, accidental roughness caused by dust and fly accretion becomes less critical with increase in altitude.*
5. *Instability of the boundary layer due to crossflow, as it occurs on swept wings, can be overcome by suitable distribution of suction and grading of its intensity.*
6. *Suction surfaces can be designed and manufactured in an engineering fashion with tolerably low weight penalties.*

The step from the present state of the art to the successful application on an economical transport aircraft is obviously still very big but there is sufficient promise that the reward is worth the effort."

Lachmann presents an analysis of the aerodynamic design considerations† for an aircraft with full laminar flow wings, followed by a discussion of weight, structural and engineering considerations, including the special requirements associated with preventing and/or removing fly accretion on the leading edge.

The article includes a detailed analysis, by Handley Page Research Department, of the reduction in direct operating costs by applying full laminar flow control to the wings, fin and tailplane of an aircraft designed for the London to New York route. The fuselage was assumed to have a fully turbulent boundary layer and was taken as identical in every respect to that of the actual aircraft design used as a comparator in the exercise. The comparison between the conventional and laminar aircraft was done for two levels of oil price ($4·8 and $3·6 per barrel at 1961 oil prices and today's $/£ exchange rate, $72 and $54 a barrel allowing for a factor of 15 price inflation since 1960)‡. The straight comparison showed DOC reductions of 21·6% and 19·2% respectively at the two oil prices. Adding in what was termed the 'maximum additional cost' for the laminar flow aeroplane brought the reductions in DOC down to 18·9% and 16·3%. This engineering study was for the HP-113 project of which the company had made a full engineering study by 1958 and which is illustrated in Ref. 46.

By the time of the HP-113, however, the performance penalty of having turbulent flow over the fuselage was thought excessive and an all laminar flying wing project, the HP-117, was put in hand. This aircraft, Fig. 20, was designed as a transatlantic airliner carrying 300 passengers and 10,000lb of freight cruising at a Mach number of 0·8. Direct operating costs were estimated to be approximately 33% lower than those of a conventional non-laminarised airliner carrying the same payload. The HP-117 was the inspiration behind the Laminar Flying Wing modelled in the Greener by Design reports[8,9], the aerodynamic characteristics being estimated, with some added conservatism, from the Northrop data from the F-94 flight tests reported in Ref. 46. The relative fuel efficiency of this type of aircraft, compared with a conventional swept-winged aircraft and one with HLFC on wings, nacelles, fin and tailplane, is shown in Fig. 21 in the form of payload fuel efficiency plotted against design range. HLFC is predicted to increase the maximum fuel efficiency by 16% and increase the most fuel efficient design range from 4,000km to 5,000km. The Laminar Flying wing is projected to increase the maximum fuel efficiency by almost 80% at a most efficient range of 7,500km. Although an element of conjecture was involved in creating the performance model for the Laminar Flying Wing, the relative efficiencies suggested by Fig. 21 are thought unlikely to be far adrift.

As to the HP-117 project, following the original proposal shown in Fig. 20 of a large flying wing passenger aircraft, Handley Page developed the concept further under government funding to meet a range of military roles – maritime patrol, nuclear deterrence and military transport‡‡. The result was an aircraft with higher aspect ratio, less wing sweep and greater span than the original passenger version. To meet its payload requirements it had a short fuselage, which enabled the thickness- chord ratio of the wing to be reduced, hence the reduced sweep. Like the civil version, directional stability and control was provided by twin fins at the wingtips – a layout first used on Lachmann's design of the propeller driven HP-75 Manx, which flew as a prototype in 1943.

More than one size of military HP-117 was considered and there was also a civil, 215 seat version of the new configuration. The case for full laminar flow for the military version of the aircraft was the greatly increased range it offered for the strategic role and the increased endurance for maritime patrol. Even with the propulsion

† Lachmann argues for discussing L/D in terms of wing span and a parameter $d_0 = D_0/q$ which is the same as the zero-lift drag area S_{DO} of Equation (10) above. In fact, he derives the same results and draws the same conclusions as in Section 4.2.2.3 of Ref. 8, but some 40 years earlier!

‡ In July 2006 the average price of crude oil was around $72 per barrel.

‡‡ In writing this paper I have been greatly helped by the loan of some Handley Page reports by Mr Harry Frazer-Mitchell, Secretary of the Handley Page Association. His address is:16 Guernsey Drive, Fleet, Hants, GU51 2TG, UK.

Table 2
Aerofoil drag comparisons

	Fully turbulent	HLFC	Fully laminar
Profile drag	0·00912	0·00595	0·00018
Pump drag	0	0·00010	0·00078
Total drag	0·00912	0·00605	0·00096

standards of 1960, the projected range of the troop carrying version of the large (400,000lb) aircraft would have enabled an unrefuelled London to Sydney flight with 100 troops on board. At a classified conference on the project in November 1962, focussing on the military versions of the HP-117, a paper by G. F. Joy, the Handley Page Chief Designer, contained a short passage on the civil version of the HP-117 which began,

"*The view is widely held that there will never be a new large long range subsonic civil transport. This opinion has probably been strengthened by recent announcements on British and French government support for the Mach 2 Supersonic Transport. On the other hand, some people think that there will be a large volume of civil traffic, including freight, which will travel subsonically for many years to come. In fact, if long range subsonic transport can be made still cheaper, it may well hold its place alongside supersonic transport practically for all time.*"

What 'some people' were said to think at that time has turned out to be true, except for the expectation of a continuing major role for supersonic air transport. And note that this prophetic view was expressed some 18 months before the US Army issued its Request for Proposal for the Heavy Logistics System (CX-HLS). This RFP led to the competition, eventually won by the Lockheed C-5A, from which the Boeing 747 also emerged as the first of the generation of wide-bodied passenger aircraft, powered by high bypass ratio turbofans, that have transformed air travel.

In the month following the HP-117 conference, President Kennedy and British Prime Minister Harold Macmillan signed an agreement under which the US would supply Polaris missiles for use in British built ballistic missile submarines and the UK need for a new, long range airborne delivery system was gone. Support for the research and demonstration programme continued, under a civil banner, with flight tests at Cranfield on a swept wing with full chord suction mounted vertically on the fuselage of Lancaster[33,34] and a joint study by Handley Page and HSA of an aircraft with fully laminarised wings, fin and tailplane, the HP-130, based on the HS 125. In the event, the design study was completed with the confident expectation that the HP-130 would show the expected performance gain but no funding was available to build the demonstrator aircraft. At about the same time, US funding for laminar flow research dried up and in August 1969 Handley Page went into voluntary liquidation, largely caused by the high development cost of the HP-137 Jetstream.

After a decade of inactivity from the mid 1960s to the 1970s, American research on laminar flow built up again followed by increased activity in Europe, albeit on a smaller scale than in the USA. The main emphasis of this work has been on HLFC and has provided further insight into some of the engineering and operational questions that had been addressed but only partly answered by the time Ref. 46 was published. One particularly significant outcome of the work led by NASA Langley is the flight test experience with a Lockheed JetStar fitted with different HLFC systems on each wing. Over a four year period, from 1983 to 1987, the aircraft was operated by NASA Dryden under conditions aimed at closely simulating routine airline operation. The experience with both LFC systems was positive in all respects[47]. Braslow[48] provides an overall account of activities in laminar flow control by suction, particularly in the USA, from the early days up to the mid 1990s.

6.3.4 Drag, suction power and propulsion

For an aerofoil with boundary-layer suction, there is a drag associated with the ingested flow. In inviscid flow, the aerofoil experiences a sink drag, equal to the rate of suction mass flow times the free-stream velocity. This is balanced by an equal thrust on the aircraft when the ingested flow is re-injected into the airstream and the net drag is zero.

In the real world, the suction flow begins, at entry to the suction hole or slot, with a total pressure equal to the local static pressure. Over most of the surface, this will be lower than the far free-stream static pressure and substantially lower than the stagnation pressure into the engine inlets. After a pressure drop through the suction surface, and possibly a further drop through some form of suction regulation system, there will be additional pressure losses in the suction ducting before the flow reaches the suction pump or pumps. The task of the pump(s) is to increase the total pressure of the suction flow sufficiently for it to be exhausted back into the free stream, through one or more propelling nozzles, at a velocity similar the exhaust velocity of the main engines.

The pumping power required, divided by the free-stream velocity, is the drag arising from the suction. This so-called pump drag depends not only on the pressure losses upstream of the pump but also on the efficiency of the pump system and that of the source of the power driving the pump. It cannot be expressed as a simple function of the total suction quantity and has to be estimated carefully in each individual case. Table 2 above shows illustrative profile and pump drags for the two aerofoils illustrated in Figs 17 and 18 and for an aerofoil based on the suction glove flight tested by Northrop on the F-94[46], all at a Reynolds number of 30×10^6 approximately.

The total drag of the HLFC aerofoil is seen to be approximately two-thirds that of the fully turbulent aerofoil while that of the fully laminar aerofoil is less than one-ninth of it. The figures in the fully laminar column are conservative estimates, being for a suction flow rate 10% higher than the flow for minimum total drag and being obtained by doubling the drags measured for the upper surface, which was the only surface to which suction was applied. No data are available for a corresponding lower surface with suction but its drag should be significantly lower than that of the upper surface.

For swept-winged HLFC aircraft, which may have HLFC applied to the wings, nacelles, fin and tailplane, the drag of the turbulent flow over the fuselage will be a greater proportion of the total profile drag and the pump drag will be only a few percent of the total aircraft drag. The system design requirements are that pressure losses ahead of the pump should be as low as practicable, the pump should have a high efficiency and total system weight should be low. Schrauf[38] has discussed these problems.

For the fully laminar aerofoil, the pump drag is more than 80% of the total profile drag and the same is likely to apply for a fully laminar aircraft. If, as in the discussion below Equation (13) above, a fully laminar aircraft is optimised to cruise below its altitude for maximum L/D such that $\lambda = 1{\cdot}25$, its drag will be split approximately 60% profile, 40% lift-dependent; pump drag will then be in the region of half the total drag. That is to say, half the propulsion comes from the suction pumping.

Lachmann discusses this in his paper in Ref. 46 and J. B. Edwards provides an extended treatment of the fundamental aspects of the problem in the same book. These contributions were written at a time when the straight-through turbojet was the propulsion norm. Some of the conclusions may be changed by the arrival of the high bypass ratio engine, but not the conclusion that the laminar flow aircraft presents a special case of the integration of lifting and propulsion systems which has to be addressed from first principles. Project design will require giving as much attention to the efficiency of processes within the suction system as is now applied to the efficiency of processes within the engine.

Figure 22 shows the large blended wing-body of the EC NACRE programme. It is not intended to include laminar flow control in the design study of this aircraft within NACRE. Nevertheless, the configuration might well lend itself to a study of full laminarisation, which would have to include integration of the power plant, at some future date.

7.0 RECAPITULATION

In the coming century, the impact of air travel on the environment will become an increasingly powerful influence on aircraft design. Unless the impact per passenger kilometre can be reduced substantially relative to today's levels, environmental factors will increasingly limit the expansion of air travel and the social benefits that it brings.

The three main impacts are noise, air pollution around airports and changes to atmospheric composition and climate as a result of aircraft emissions at altitude. Of the three, impact on the atmosphere and climate is the most important in the long term

There are three main contributors to climate change from aviation, the emission of CO_2 and NO_x and the formation of persistent contrails and cirrus cloud.

There is only one way to reduce contrail and contrail-cirrus formation, which is to route air traffic below, above or around regions of cold, moist air. This will increase fuel burn and disrupt airline schedules but, in the long run, that may be a price that has to be paid.

Emission of NO_x per tonne of fuel burned can be reduced by technological advances in engine and combustor design. Substantial improvements have been achieved in technology demonstrator programmes and further improvements are expected from demonstrator programmes that are now in train.

Reducing fuel burn is the only way of reducing the third impact, CO_2 emissions. This has long been a key commercial objective and now, as pressures to reduce the impact of aviation on climate increase, it is becoming a key environmental objective. Most advances which reduce fuel burn will also reduce NO_x emissions.

What can be achieved in this respect is finite. It is circumscribed by the 'Laws of Physics'. There is, for example, no escaping the Breguet range equation.

The effect of design range was discussed in 4.2.1. For the long haul end of the market, significant fuel burn reduction could be achieved by a change to multi-stage flights in aircraft designed for ranges between 5,000 and 7,500km. In Ref. 8 it was estimated that universal adoption of this might reduce total world fuel burn by 6% (though on the basis of Refs 10 and 11 this estimate might now increase to 9-10%). Further reduction in fuel burn can be achieved though more efficient routing, possibly as much as 10% eventually. Reducing aircraft weight is one of the most powerful means of reducing fuel burn. It is difficult to suggest a limit here on what might be possible in the longer term as a result of advances in materials and structural design – there does not appear to be an equivalent to the Second Law of Thermodynamics on which we can call to define a boundary.

In seeking improvements in propulsion efficiency, on the other hand, we do know that there is a boundary, set by the Second Law, which we have been steadily approaching over the last 40 years. There is at present still room for improvement – studies have suggested a possible further 30% improvement before the theoretical limit is reached – but there are likely be great technical difficulties as the limit is approached. A projected ultimate improvement in the range 20% – 25% is probably a more realistic expectation[9].

The last card in our hand, and potentially the highest, is increasing the lift to drag ratio at cruise. Here we are circumscribed, not by the Second Law but by physical principles and by aspects of the behaviour of real fluids that Lanchester saw clearly in the late nineteenth century, even though he did not publish his ideas until 1907.

He was the first to understand that a finite lifting wing had a drag arising from the energy lost in the vortices trailing from its wing tips, that an aircraft also had drag arising from skin friction and flow separations, and that it is at its most aerodynamically efficient when these two drag terms are equal. That is one of the facts that we cannot avoid and it remains central to civil aircraft design optimisation.

Following Prandtl's more rigorous mathematical treatment of the subject, we know that the two main ways we have to improve aerodynamic efficiency – i.e. to increase *L/D* – is to increase wing span and reduce profile drag area.

Current aircraft are close to an optimum in the trade-off between reducing drag and increasing weight as span is increased. Advances in structural materials and other possibilities discussed in Ref. 9 offer some prospects for further improvement, but the resultant increases in *L/D* are likely to be relatively modest.

This leaves the reduction of profile drag area as the outstanding option, in both senses of the word, although here again we run into a limit that Lanchester foresaw a century ago. He developed his own concept of the boundary layer, formulated a mathematical model for its skin friction in laminar flow, proposed a different model for the friction law in turbulent flow and understood that the experiments of Reynolds, showing the breakdown of laminar into turbulent flow, were of fundamental importance to an understanding of the difference. He went on to propose Reynolds number as a means of defining dynamic similarity and assumed that aircraft operate in the turbulent regime.

Lanchester's assumption applies pretty well to today's transport aircraft, all of which fly with turbulent boundary layers over virtually their entire surface. This reflects the aspect of the behaviour of real, viscous fluids that Reynolds demonstrated in his pipe experiments in 1883; that above a certain Reynolds number, the flow becomes unstable and a laminar boundary layer undergoes transition into a turbulent one. Instability of a laminar boundary layer, and the turbulent flow that follows, is another of the 'Facts of Life'.

A consequence of this is that, for the classic, highly developed, swept-winged transport aircraft, there is very limited scope for reducing the profile drag area if the boundary layer over the entire surface remains turbulent, as it is today. There is, however, scope for significant drag reduction if laminar flow can be maintained over some key sections of the aircraft.

An important aspect of laminar boundary-layer behaviour is that its stability can be substantially increased, and transition delayed, by flow acceleration or surface suction. This is a feature of the behaviour of a real fluid – a 'Fact of Life', but a helpful one that makes possible drag reduction by laminar flow control.

Natural laminar flow control and hybrid laminar flow control both work by maintaining the boundary layer in a laminar condition over the forward part of an aerofoil upper surface, thereby reducing skin friction and boundary-layer growth up to mid-chord. To this is added the further, substantial benefit of the consequential reduction in boundary-layer growth in the rising pressure field over the rear of the aerofoil. The result can be a reduction in aerofoil drag by one-third or more. The same techniques can be applied to tail surfaces and nacelles with similar effect. These are the forms of control that have been most actively considered for aircraft in the past forty years. They offer reductions in fuel burn of the order of 15%, but that is about as much as they can achieve.

We come finally to full laminar flow control. It is the last, and the ultimate, aerodynamic option. It can be achieved only by all-over surface suction on surfaces which are free from bumps and protuberances. An aircraft in which full laminar flow control is integrated with a propulsion system that is as efficient as the technology of the day allows will represent the limit of what is achievable in terms of aerodynamic and propulsion efficiency. And whilst the approach of the propulsion system to the limit set by the Second Law will be slow and difficult, I suggest that the approach to the aerodynamic limit need not be so protracted. Moreover, the rewards of making this step – and it is really a leap rather than a step – are far greater than those that can be expected from the continued advance of engine technology.

The research and flight tests in the 1950s confirmed that full-chord laminar flow is achievable and the work since then, particularly in the USA, has increased confidence that the practical obstacles to achieving it can be overcome. We know where the limits set by the 'Laws of Nature' are and how, in principle, we can reach them. Getting there is just a matter of engineering. There is no fundamental barrier and the task is for the aerodynamicists, supported by the structural and systems engineers and the material scientists, to take us forward. Were the young Lanchester with us today, he would be just the man to lead the way.

REFERENCES

1. ACKROYD, J.A.D. Lanchester – The Man, *Aeronaut J*, April 1992, **96**, (954), pp 119-140.
2. KINGSFORD, P.W. *F.W. Lanchester – A Life of an Engineer*, Edward Arnold, London, UK, 1960.
3. LANCHESTER, F.W. *Aerodynamics*, Constable & Co, London, UK, 1907.
4. LANCHESTER, F.W. *Aerodonetics*, Constable & Co , London, UK, 1908.
5. LANCHESTER, F.W. The flying machine: the aerofoil in the light of theory and experiment, *Proc Inst Auto Eng*, 1915, **9**, pp 171-259.
6. LANCHESTER, F.W. *Aircraft in Warfare*, Constable & Co Ltd, London, UK, 1916.
7. KARMAN, T. von. Lanchester's contributions to the theory of flight and operational research, *J R Aeronaut Soc*, 1958, **62**, pp 80-93.
8. GREEN, J.E. Greener by Design – the technology challenge, *Aeronaut J*, February 2002, **106**, (1056), pp 57-113.
9. GREEN, J.E. Air Travel – Greener by Design – Mitigating the environmental impact of aviation: Opportunities and priorities, *Aeronaut J*, September 2005, **109**, (1099), pp 361-416.
10. NANGIA, R.K. Efficiency parameters for modern commercial aircraft, *Aeronaut J*, August 2006, **110,** (1110). pp 495-510
11. GREEN, J.E. Küchemann's weight model as applied in the first Greener by Design Technology Sub Group report: a correction, adaptation and commentary, *Aeronaut J*, August 2006, **110,** (1110). pp 511-516.
12. Department for Transport, Aviation and the environment: using economic instruments, March 2003.
13. Intergovernmental Panel on Climate Change*, Aviation and the Global Atmosphere*, Cambridge University Press, 1999.
14. SAUSEN, R., ISAKSEN, I., GREWE, V., HAUGLUSTAINE, D., LEE, D.S., MYHRE, G., KÖHLER, M.O., PITARI, G., SCHUMANN, U., STORDAL, F. and ZEFEROS, C. Aviation radiative forcing in 2000: An update on IPCC (1999), *Meteorol Z*, **14**, (4), pp 555-561
15. ROGERS, H.L., LEE, D.S., RAPER, D.W., FOSTER, P.M.DEF., WILSON, C.W. and NEWTON, P.J. The impacts of aviation on the atmosphere, *Aeronaut J*, October 2002, **104**, (1064), pp 521-546.
16. MANNSTEIN, H. and SCHUMANN, U. Aircraft induced contrail-cirrus over Europe, *Meteorol Z*, 2005, **14**, pp 549-554.
17. WILLIAMS, V. and NOLAND, R.B. Variability of contrail formation conditions and the implications for policies to reduce the climate impacts of aviation, *Transportation Research Part D*, 2005, **10**, pp 269-280.
18. GAUSS, M., ISAKSEN, I., GREWE, V., KÖHLER, M., HAUGLUSTAINE, D. and LEE, D. Impact of aircraft NO_x emissions: effect of changing the flight altitude, Proceedings of EC conference Aviation, Atmosphere and Climate, Friedrichshafen, Germany, 30 June – 3 July 2003, EOR 21051.
19. KLUG, H.G., BAKAN, S. and GAYLER, V. Cryoplane – Quantitative comparison of contribution to anthropogenic greenhouse effect of liquid hydrogen aircraft versus conventional kerosene aircraft, European Geophysical Society, XXI General Assembly, The Hague, The Netherlands, May 1996.
20. BIRCH, N.T. 2020 Vision: The prospects for large civil aircraft propulsion, *Aeronaut J*, August 2000, **104**, (1038), pp 347-352.
21. WHELLENS, M.W. and SINGH, R. Propulsion system optimisation for minimum global warming potential, Proceedings of ICAS 2002 Congress, Toronto, Canada, September 2002, Paper 7111.
22. LANCHESTER, F.W. Aerofoils of high aspect ratio, Advisory Committee for Aeronautics, R&M, (109), 1913.
23. PRANDTL, L. Tragflügeltheorie, I Mitteilungen, *Nachr Ges Wiss Göttingen,* Maths-Phys K1, 1918, pp 451-477.
24. REYNOLDS, O. An experimental investigation of the circumstances which determine whether the motion of water shall be direct or sinuous and of the law of resistance in parallel channels, *Phil Trans R Soc A*, 1883, **174**, pp 933-982.
25. KÜCHEMANN, D. *The Aerodynamic Design of Aircraft*, Pergamon, 1978.
26. MAREC, J-P. Drag reduction: a major task for research, CEAS/DragNet European Drag Reduction Conference 2000, Potsdam, Germany June 2000.
27. PRANDTL, L. Über Flüssigkeitsbewegung bei sehr kleiner Reibung, Verhandlungen des dritten internationalen Mathematiker-Kongresses, 1904, Heidelberg, Leipzig, Germany.
28. RAYLEIGH, Lord (STRUTT, J.W.) On the stability or instability of certain fluid motions, *Proc Lond Matth Soc,* **11**, (1880), pp 57-70 (see also Tollmien and Grohne, Ref. 30 below).
29. TOLLMIEN, W. Über die Entstehung der Turbulenz, I Mitteilung, *Nachr Ges Wiss Göttingen*, Math-Phys Kl, 1929, pp 21-44. Translation: NACA TM No. 609 (1931).
30. TOLLMIEN, W. and GROHNE, D. The Nature of Transition*, Boundary Layer and Flow Control,* Lachmann, G.V., **2**, Pergamon, 1961.
31. OWEN, P.R. and RANDALL, D.G. Boundary layer transition on a swept back wing, 1952, RAE Technical Memorandum No Aero 277 and 1953, RAE Technical memorandum No 330.
32. PFENNINGER, E. Some results from the X21 program. Part I: Flow phenomena at the leading edge of swept wings, Recent Developments in Boundary Layer Research, Part IV, May 1965, AGARDograph 97.
33. GASTER, M. A simple device for preventing turbulent contamination of swept leading edges, *Aeronaut J*, 1965, **69**, pp 788-789.
34. GASTER, M. On the flow along swept leading edges, *Aeronaut J*, 1965, **69**, p 788.
35. POLL, D.I.A. Some observations of the transition process on the windward face of a long yawed cylinder, *J Fluid Mech*, 1985, **150**, pp 329-356.
36. ARNAL, D. Boundary layer transition. Predictions based on linear theory, April 1994, Special Course on Progress in Transition Modelling, AGARD Report 793.
37. WONG, P.W.C. and MAINA, M. Flow control studies for military aircraft applications, AIAA 2nd Flow Control Conference, Portland, Ore, 2004, AIAA 2004-2313.
38. SCHRAUF, G. Status and perspectives of laminar flow, *Aeronaut J*, December 2005, **109**, (1102), pp 639-644.
39. BLASIUS, P.R.H. Grenzschichten in Flüssigkeiten mit kleiner Reibung, *Z für Mathematik und Physik*, 1908, **56**, pp1-37.
40. PRETSCH, J. Die Stabilität einer ebenen Laminarströmung bei Druckgefälle und Druckandstieg, *Jb dtsch Luftfahrtforsch*, 1941, 1, pp 58-75.
41. HEAD, M.R. Methods of Calculating the Two Dimensional Laminar Boundary-Layer, *Boundary Layer and Flow Control,* Lachmann, G.V., **2**, Pergamon, 1961.
42. Boeing Commercial Airplane Company, Natural laminar flow airfoil analysis and trade studies, NASA Contractor Report 159029, May 1979.
43. BUSSMAN, K AND MÜNTZ, H. Die Stabilität der laminaren Reibungsschicht mit Absaugung, *Jb dtsch Luftfahrt*, 1942, **1**, pp 1-7.
44. ASHILL, P.R., WOOD, R.F. and WEEKS, D.J. An Improved, Semi-Inverse Version of the Viscous Garabedian and Korn Method (VGK), RAE TR 87002, 1987.
45. SCHRAUF, G. AND KÜHN, W. Industrial aspects of laminar flow, presented at EC Fourth Aeronautics Days, Hamburg, Germany, January 2001.
46. LACHMANN, G.V. (Ed) *Boundary Layer and Flow Control*, **2**, Pergamon, 1961.
47. MADDALON, D.V. and BRASLOW, A.L. Simulated-airline service flight tests of laminar-flow control with perforated-surface suction system, NASA Technical Paper 2966, Washington DC, USA, March 1990.
48. BRASLOW, A.L. *A History of Suction-Type Laminar-Flow Control with Emphasis on Flight Research*, NASA History Division, Monographs in Aerospace History No. 13, Washington DC, USA, 1999.